Fractals, Vol. 16, No. 1 (2008) 43–68

World Scientific
www.worldscientific.com

SPECTRA OF SELF-SIMILAR LAPLACIANS ON THE SIERPINSKI GASKET WITH TWISTS

ANNA BLASIAK* and ROBERT S. STRICHARTZ†,‡
*Computer Science Department
and
†Mathematics Department, Malott Hall
Cornell University, Ithaca, NY 14853, USA
*ablasiak@cs.cornell.edu
†str@math.cornell.edu

BARIS EVREN UGURCAN
Matematik Bolumu, Bilkent Universitesi
06800 Bilkent/Ankara, Turkey
ugurcan@alumni.bilkent.edu.tr

Received May 29, 2007
Accepted June 15, 2007

Abstract

We study the spectra of a two-parameter family of self-similar Laplacians on the Sierpinski gasket (SG) with twists. By this we mean that instead of the usual IFS that yields SG as its invariant set, we compose each mapping with a reflection to obtain a new IFS that still has SG as its invariant set, but changes the definition of self-similarity. Using recent results of Cucuringu and Strichartz, we are able to approximate the spectra of these Laplacians by two different methods. To each Laplacian we associate a self-similar embedding of SG into the plane, and we present experimental evidence that the method of outer approximation, recently introduced by Berry, Goff and Strichartz, when applied to this embedding, yields the spectrum of the Laplacian (up to a constant multiple).

Keywords: Sierpinski Gasket; Laplacians on Fractals; Spectrum; Outer Approximation; Twists.

‡Corresponding author.

1. INTRODUCTION

Kigami[1] gives a general construction of self-similar energies and Laplacians on a family of self-similar fractals that includes the familiar Sierpinski gasket (SG), the invariant set for the iterated function system (IFS) consisting of three homothetic similarities $\{F_i\}$ with contraction ratio $\frac{1}{2}$ and fixed points $\{q_i\}$, the vertices of an equilateral triangle in the plane. Sabot[2] gives a complete description of all possible self-similar energies on SG. Recently, Cucuringu and Strichartz[3] revisit the problem using a different IFS denoted $\{\tilde{F}_i\}$, where each $\tilde{F}_i$ is the composition of F_i with the reflection that fixes q_i and permutes the other two vertices of the triangle. This IFS has the same invariant set SG, but we refer to it informally as SG with twists. The set of self-similar energies with respect to $\{\tilde{F}_i\}$ is not the same, and it turns out that it has a much simpler and completely constructive description. In addition, there is a family of self-similar embeddings of SG with twists in the plane that are all given by IFSs that are topologically conjugate to $\{\tilde{F}_i\}$, but with the contraction ratios different from $(\frac{1}{2}, \frac{1}{2}, \frac{1}{2})$. (Without the twists this is simply impossible.) The purpose of this paper is to study the spectra of families of the self-similar Laplacians naturally associated to the self-similar energies on one hand, and the self-similar embeddings on the other hand, using the method of outer approximation introduced in Berry *et al.*[4] Both families of Laplacians have two parameters, and we propose a one-to-one correspondence between the parameters that we conjecture will make the two Laplacians equal (up to a constant).

We begin with a brief review of Kigami's construction (see also Refs. 5 and 6). Suppose K is a connected non-empty compact set satisfying

$$K = \bigcup F_i K \tag{1.1}$$

for some IFS $\{F_i\}$ (for simplicity we assume these are contractive similarities on some Euclidean space). We write $F_w = F_{w_1} \circ \cdots \circ F_{w_m}$ for a word $w = (w_1, \ldots, w_m)$ of length $|w| = m$, and call $F_w K$ a *cell* of level m. We say that K is *post-critically finite* (PCF) if there exists a finite subset $V_0 \subseteq K$, called the *boundary* of K, such that

$$F_w K \cap F_{w'} K \subseteq F_w V_0 \cap F_{w'} V_0 \tag{1.2}$$

whenever w and w' are distinct words of the same length. We consider $F_w V_0$ to be the boundary of the cell $F_w K$. Thus (1.2) says that distinct cells of the same level intersect only at points on their boundary. Because we assume K is connected, there must be enough non-empty intersections. SG is perhaps the simplest non-trivial example (the unit interval is a trivial example).

We then approximate K by a sequence of graphs $\{\Gamma_m\}$ with vertices $\{V_m\}$ and edge relation $x \underset{m}{\sim} y$ as follows: Γ_0 is the complete graph on V_0, and Γ_m is defined inductively as the image of Γ_{m-1} under the IFS with the appropriate vertices identified. For simplicity we assume that each vertex in V_0 is the fixed point of one of the IFS mappings, say $F_i q_i = q_i$ (in general there may be more mappings in the IFS than vertices in V_0). Then $V_0 \subseteq V_1 \subseteq V_2 \subseteq \cdots$. Figure 1 shows Γ_m for $m = 0, 1, 2$ for the standard SG, and Fig. 2 shows the same for SG with twists. We consider graph energies $\mathcal{E}_m$ on Γ_m. These are nonnegative bilinear forms on the functions on V_0 that are zero exactly on the constants. We write $\mathcal{E}_m(u) = \mathcal{E}_m(u, u)$ for the associated quadratic form, that determines the bilinear form via polarization identity $\mathcal{E}_m(u, v) = \frac{1}{4}\big(\mathcal{E}_m\big(\frac{u+v}{2}\big) - \mathcal{E}_m\big(\frac{u-v}{2}\big)\big)$. We require

$$\mathcal{E}_m(u) = \sum_{x \underset{m}{\sim} y} c(x, y)\,(u(x) - u(y))^2 \tag{1.3}$$

for certain positive conductances $c(x, y)$ (we may interpret the reciprocals $c(x, y)^{-1}$ as resistances, and think of the graph as representing an electric network of resistors with resistances $c(x, y)^{-1}$ on each edge). This not only guarantees the nonnegativity of the form, but also the Markov property $\mathcal{E}_m(\overline{u}) \leq \mathcal{E}_m(u)$ for $\overline{u}(x) = \min\{\max\{u(x), 0\}, 1\}$. We also want two compatibility relations to hold for this family of energies. The first is that $\mathcal{E}_{m-1}$ should be the *restriction* of $\mathcal{E}_m$ to Γ_{m-1}, defined as follows:

$$\mathcal{E}_{m-1}(u) = \min \mathcal{E}_m(\tilde{u}) \tag{1.4}$$

where the minimum is taken over all $\tilde{u}$ satisfying $\tilde{u}\,|_{V_{m-1}} = u$ (it is easy to see that a unique minimum exists, and the extension $\tilde{u}$ that achieves the minimum is called the *harmonic extension*). The second condition is the self-similarity condition

$$\mathcal{E}_m(u) = \sum_i r_i^{-1} \mathcal{E}_{m-1}(u \circ F_i) \tag{1.5}$$

for a set of *resistance renormalization factors* $\{r_i\}$ satisfying $0 < r_i < 1$. It is easy to see that the initial energy on Γ_0, which can be written

$$\mathcal{E}_0(u) = \sum_{i<j} c_{ij}(u(q_i) - u(q_j))^2, \tag{1.6}$$

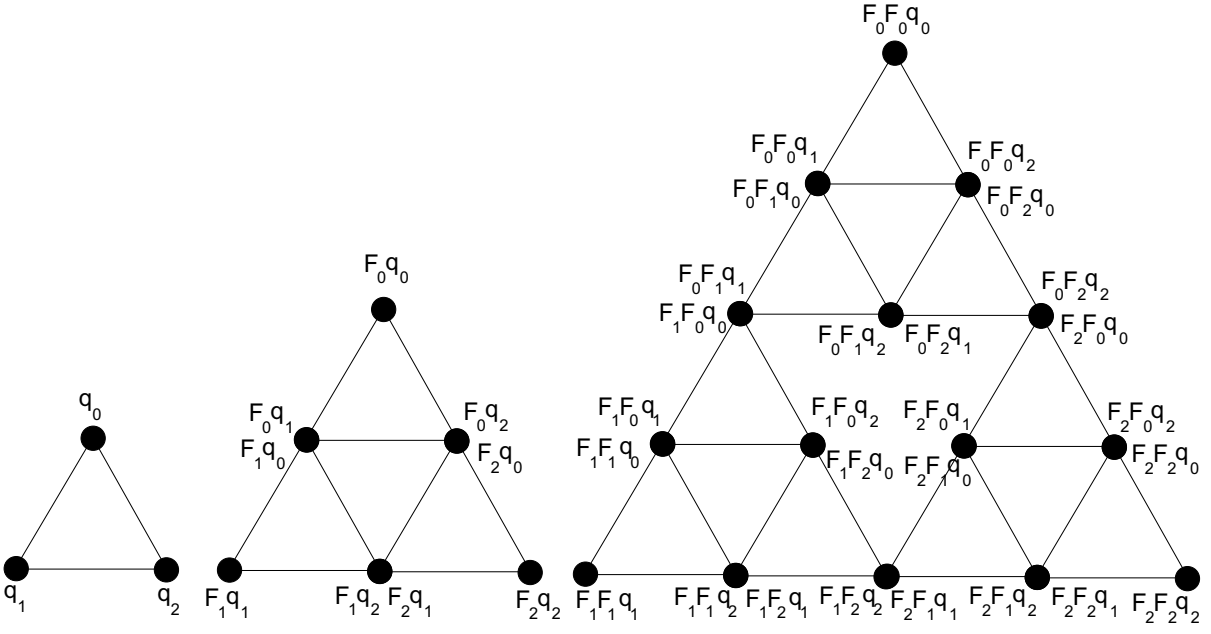

Fig. 1 $\Gamma_0, \Gamma_1, \Gamma_2$ for the standard SG.

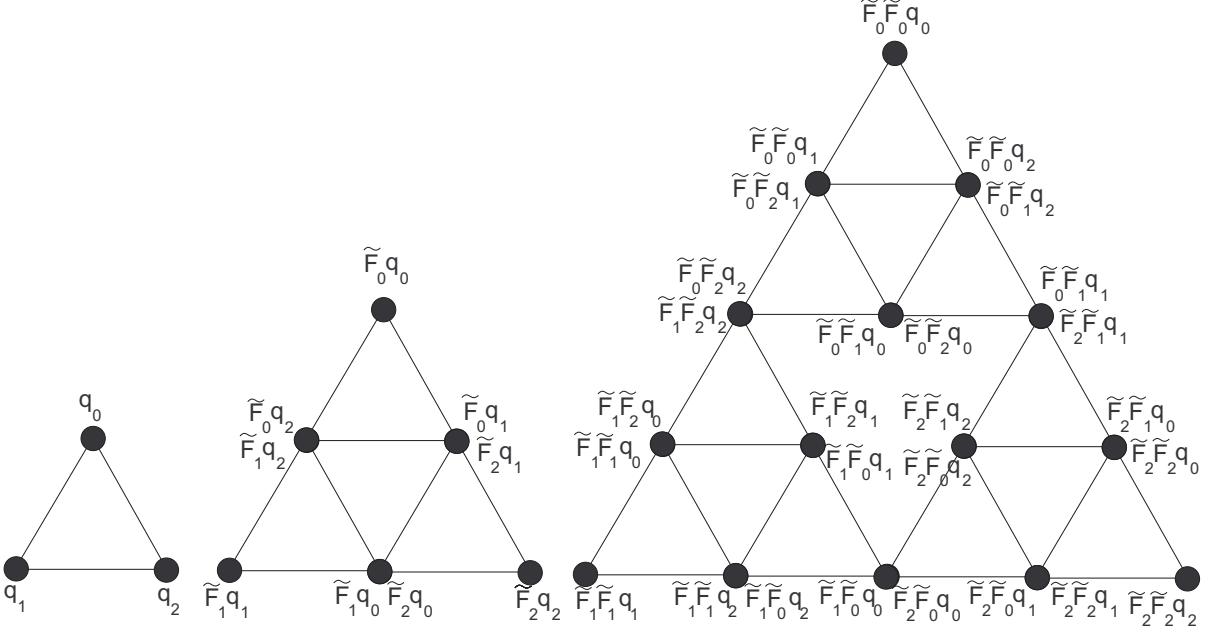

Fig. 2 $\Gamma_0, \Gamma_1, \Gamma_2$ for SG with twists. Note that the two labels for each have the same q_j.

and the $\{r_i\}$ determine all Γ_m inductively via (1.5), and so the question becomes whether or not (1.4) holds. It is also easy to see that it suffices to check (1.4) for $m = 1$, and if so then it holds for all m by induction. We refer to (1.4) for $m = 1$ as the *renormalization equation*. The existence of solutions to the renormalization equation is a highly non-trivial problem, and it requires a careful balancing of the initial conductances and the resistance renormalization factors.

Given a solution to the renormalization equation, it is easy to construct a limiting energy on K:

$$\mathcal{E}(u) = \lim_{m\to\infty} \mathcal{E}_m(u) \tag{1.7}$$

because the sequence $\{\mathcal{E}_m(u)\}$ is always monotone increasing. We define the domain $\operatorname{dom}\mathcal{E}$ to be the set of continuous functions on K for which $\mathcal{E}(u)$ is finite. It can be shown that $\operatorname{dom}\mathcal{E}$ modulo constants forms a Hilbert Space with inner product $\mathcal{E}(u,v)$. The fact the $\operatorname{dom}\mathcal{E}$ is entirely contained in the space of continuous functions is one of a constellation of equivalent properties described as "points have positive capacity." This property does not hold for the standard energy on Euclidean domains in dimensions greater than one. It follows from (1.5) that the energy $\mathcal{E}$ on K is self-similar:

$$\mathcal{E}(u) = \sum_i r_i^{-1}\,\mathcal{E}(u\circ F_i). \tag{1.8}$$

To define a Laplacian we need two ingredients: an energy $\mathcal{E}$ and a measure μ. (Note that in Riemannian geometry, both are derived from the Riemannian metric, but there is no analogous concept on fractals, and the measure and energy do not have to be related.) We will consider only *self-similar measures*, satisfying the identity

$$\mu = \sum_i \mu_i \mu\circ F_i^{-1} \tag{1.9}$$

for a finite set of probabilities $\{\mu_i\}$. In fact we will make the choice

$$\mu_i = r_i^{\alpha} \tag{1.10}$$

for the unique α that yields the probability condition

$$\sum_i r_i^{\alpha} = 1. \tag{1.11}$$

Note that this means the parameters $\{\log r_i\}$ and $\{\log \mu_i\}$ are proportional. The Laplacian Δ is defined as follows. We say $u\in\operatorname{dom}\Delta$ and $\Delta u = f$ if $u\in\operatorname{dom}\mathcal{E}$, f is continuous, and

$$\mathcal{E}(u,v) = -\int_K f v\,d\mu \quad \forall v\in \operatorname{dom}_0\mathcal{E}, \tag{1.12}$$

where $\operatorname{dom}_0\mathcal{E}$ denotes the subset of $\operatorname{dom}\mathcal{E}$ of functions vanishing on V_0. Moreover, we say that u belongs to the domain of the *Neumann Laplacian* if (1.12) holds for all $v\in\operatorname{dom}\mathcal{E}$. It is possible to describe the Neumann domain in terms of vanishing of certain normal derivatives of u on the boundary, but we prefer the above "natural" description. The Neumann Laplacian has a complete set of eigenfunctions $\{u_j\}$ with eigenvalues $\{\lambda_j\}$ satisfying

$$0 = \lambda_0 < \lambda_1 \le \lambda_2 \le \cdots \to \infty. \tag{1.13}$$

This is the spectrum that we study.

The main result of Cucuringu and Strichartz[3] is that the renormalization problem for SG with twists has a solution for any projective choice of resistance renormalization factors. That is, given any vector $(\tilde r_0,\tilde r_1,\tilde r_2)$ in the positive octant in $\mathbb{R}^3$, there exists a unique $\lambda>0$ such that $(r_0,r_1,r_2)=\lambda(\tilde r_0,\tilde r_1,\tilde r_2)$ allows a solution for a unique (up to a constant multiple) set of initial conductances. The formula for λ and $\{c_{jk}\}$ is explicit (involving the solution of a fourth degree polynomial), and the set of all solutions (r_0,r_1,r_2) forms a portion of an explicit algebraic variety of degree six (a set defined by a polynomial equation of degree six). The choice $(r_0,r_1,r_2)=(\frac{3}{5},\frac{3}{5},\frac{3}{5})$ yields the standard energy (all c_{jk} equal) and Laplacian and this is the same with or without twists. Altogether we get a two-parameter family of Laplacians (we can take $\tilde r_0=1$ and then use $\tilde r_1,\tilde r_2$ as parameters). In Sec. 2 we describe two different methods to approximate the spectra of these Laplacians, and we present numerical data in some cases. As predicted in Kigami and Lapidus,[7] there is a difference between the *lattice case*, where there exists r such that $r_i = r^{k_i}$ for integers k_i (in other words, the values $\log r_i$ lie in a lattice subgroup of the reals), and the *non-lattice case*, everything else. The eigenvalue counting function

$$N(x) = \#\{j : \lambda_j \le x\} \tag{1.14}$$

has roughly a power growth x^{β}, for β the solution of

$$\sum_i (r_i\mu_i)^{\beta} = 1, \tag{1.15}$$

but in the non-lattice case we actually have a positive limit for the Weyl ratio $W(x) = N(x)/x^{\beta}$, while in the lattice case we have the asymptotics

$$W(x) = \psi(x) + o(1) \quad x\to\infty \tag{1.16}$$

where ψ is multiplicatively periodic

$$\psi(rx) = \psi(x) \tag{1.17}$$

and bounded on both sides

$$0 < c_1 \le \psi(x) \le c_2 < \infty. \tag{1.18}$$

In the case of the standard Laplacian we know that the function ψ is discontinuous, since we can identify a countable set of jump discontinuities corresponding to eigenvalues of high multiplicity. We have some evidence for the same behavior in the general lattice case, even though the highest multiplicity appears to be 1.

It is also mentioned in Cucuringu and Strichartz[3] that there is a two-parameter family of self-similar embeddings of SG with twists in the plane. Start with any acute triangle, with vertices denoted q_0, q_1, q_2 and corresponding angles $\alpha_0, \alpha_1, \alpha_2$. Let $\tilde{F}_i$ denote the composition of the direct similarity with fixed point q_i and contraction ratio $\cos\alpha_i$ (denoted ρ_i), and the reflection with fixed point q_i interchanging the two sides of the triangle that meet at q_i. Then the invariant set for the IFS $\{\tilde{F}_i\}$ is homeomorphic to SG with twists, although it is geometrically quite different from the standard realization (all $\rho_i = \frac{1}{2}$). Again, the parameters (ρ_0, ρ_1, ρ_2) lie on an algebraic variety, namely

$$\rho_0^2 + \rho_1^2 + \rho_2^2 + 2\rho_0\rho_1\rho_2 = 1. \tag{1.19}$$

Now, given a self-similar Laplacian with parameters (r_0, r_1, r_2) we associate the embedding with parameters (ρ_1, ρ_2, ρ_3) determined by the condition

$$\rho_i = r_i^\gamma \quad \text{for some } \gamma. \tag{1.20}$$

Note that if we substitute (1.20) in (1.19) we obtain

$$r_0^{2\gamma} + r_1^{2\gamma} + r_2^{2\gamma} + 2(r_0r_1r_2)^\gamma = 1, \tag{1.21}$$

which we can solve uniquely for γ. This choice has the property that it preserves the lattice/nonlattice dichotomy: if $r_i = r^{k_i}$ then $\rho_i = (r^\gamma)^{k_i}$ for the same set of integers. Also, the Hausdorff measure of the embedded K is a constant multiple of the self-similar measure determined by (1.10). For these reasons, we believe the correspondence (1.20) is natural. The main conjecture of this paper is that the method of *outer approximation*, applied to the embedding of K, yields the spectrum of the self-similar Laplacian (up to a constant multiple).

The method of outer approximation, introduced recently in Berry *et al.*[4] involves approximating the embedded K by a nested sequence of connected domains Ω_n in the plane, so that $K = \bigcap_n \overline{\Omega}_n$ in some reasonable way. Then consider the ordinary Neumann Laplacian Δ_n on Ω_n, and denote by $\{\lambda_j^{(n)}\}$ its spectrum. For certain renormalization factors s_n, we would like to have

$$\lim_{n\to\infty} s_n\lambda_j^{(n)} = c\lambda_j. \tag{1.22}$$

We will present numerical evidence that this is indeed true. Note that we are not suggesting that the limit is uniform across the whole spectrum. Indeed this would be impossible, since $\{\lambda_j^{(n)}\}$ obeys the Weyl asymptotic law for a two-dimensional domain. What we do see is that some initial segment of the spectra $\{\lambda_j^{(n)}\}$ and $\{\lambda_j\}$ are very close (after multiplying by a constant) for the relatively small values of n that we can handle computationally, and the size of this segment increases as we increase n. Even as the numerical values begin to diverge, other qualitative features of the two spectra seem to agree. In Sec. 3 we describe in detail our construction of the approximating regions Ω_n. This is a non-trivial problem, because the obvious domains obtained by deleting triangles from the original triangle are disconnected. In fact, the method we use here is an improvement over the method used in Berry *et al.*[4] in that it yields much greater accuracy even in the case of the standard embedding. In Sec. 4 we present data comparing the two spectra. In Sec. 5 we discuss some interesting features of the spectra we have observed, and pose some problems for future research.

Related ideas have been studied in the context of quantum graphs (see Kuchment and Zeng[8] and the references therein).

2. COMPUTING THE SPECTRUM OF A SELF-SIMILAR LAPLACIAN

Fix the values (r_0, r_1, r_2) and associated $\{c_{ij}\}$, and consider the Laplacian defined by (1.12). The first method we use for computing its spectrum is based on what we call the *pointwise formula* of Kigami. Let $\psi_x^{(m)}$ denote the piecewise harmonic function on level m satisfying

$$\psi_x^{(m)}(y) = \delta_{xy} \quad \text{for all } y \in V_m. \tag{2.1}$$

In other words, $\psi_x^{(m)}$ minimizes energy among all functions satisfying (2.1). If we put $v = \psi_x^{(m)}$ in (1.12) we obtain

$$\int_K (\Delta u)\psi_x^{(m)}\, d\mu = \sum_{x \underset{m}{\sim} y} c(x,y)(u(y) - u(x)) \tag{2.2}$$

(this uses (1.3) and the fact that $\mathcal{E}(u, \psi_x^{(m)}) = \mathcal{E}_m(u, \psi_x^{(m)})$). We approximate the left side of (2.2) by $\Delta u(x)\mu_m(x)$ for

$$\mu_m(x) = \int \psi_x^{(m)}\, d\mu. \tag{2.3}$$

This leads us to define a graph Laplacian on Γ_m by

$$\Delta_m u(x) = \mu_m(x)^{-1} \sum_{x \underset{m}{\sim} y} c(x,y)(u(y) - u(x)). \tag{2.4}$$

(for $x \in V_m \backslash V_0$ there are four summands, and for $x \in V_0$ there are two summands). For $u \in \operatorname{dom} \Delta$ it follows that

$$\Delta u = \lim_{m \to \infty} \Delta_m u \quad \text{on } V^* \backslash V_0 \tag{2.5}$$

where $V^* = \bigcup V_m$, and the limit is uniform. Note that Δ_m is a self-adjoint operator with respect to the inner product

$$\langle u, v \rangle_m = \sum_{x \in V_m} u(x) v(x)\, \mu_m(x), \tag{2.6}$$

so it is represented by a symmetric matrix, hence it has a complete set of eigenvectors. Since $-\Delta_m$ is non-negative we write

$$-\Delta_m u_j^{(m)} = \lambda_j^{(m)} u_j^{(m)} \quad \text{with} \tag{2.7}$$

$$0 = \lambda_0^{(m)} < \lambda_1^{(m)} \le \cdots \le \lambda_{N_m}^{(m)} \tag{2.8}$$

(here $N_m + 1 = \#V_m$). The functions $u_j^{(m)}$ are initially defined only on V_m, but we may extend them to be piecewise harmonic on K. The spectrum (1.13) on K is then given by

$$\lambda_j = \lim_{m \to \infty} \lambda_j^{(m)}. \tag{2.9}$$

Experimental evidence indicates that this is an increasing limit. For the standard Laplacian $(r_0, r_1, r_2) = (\frac{3}{5}, \frac{3}{5}, \frac{3}{5})$, the graph eigenvalues $\lambda_j^{(m)}$ may also be described by the method of spectral decimation, which easily implies that (2.9) is increasing. We do not know an argument for this in the general case. It is also true that the eigenfunctions $u_j^{(m)}$ converge to the eigenfunctions u_j on K, provided one makes reasonable choices of $u_j^{(m)}$.

It is straightforward to compute the spectrum of the sparse symmetric matrix Δ_m (provided we do not take the value of m too large). The values of the conductances $c(x,y)$ are determined by (1.5) and (1.6), explicitly

$$c(F_w q_i, F_w q_j) = r_w^{-1} c_{ij} \quad \text{if } |w| = m, \tag{2.10}$$

where $r_w = r_{w_1} \cdots r_{w_m}$. We also need to compute the values for $\mu_m(x)$. Note that each $\psi_x^{(m)}$ is supported on two m-cells for $x \in V_m \backslash V_0$, and one m-cell for $x \in V_0$. In the first case, if $x = F_w q_j = F_{w'} q_{j'}$, then by self-similarity

$$\int \psi_x^{(m)}\, d\mu = \mu_w \int \psi_{q_j}^{(0)}\, d\mu + \mu_{w'} \int \psi_{q'_j}^{(0)}\, d\mu, \tag{2.11}$$

where $\mu_w = \mu_{w_1} \cdots \mu_{w_m}$. In the second case

$$\int \psi_{q_j}^{(m)}\, d\mu = (\mu_j)^m \int \psi_{q_j}^{(0)}\, d\mu. \tag{2.12}$$

This reduces the problem to the $m = 0$ case; in other words, the integration of harmonic functions.

We solve this problem using self-similarity, namely

$$\int \psi_{q_j}^{(0)}\, d\mu = \sum_i \mu_i \int \psi_{q_j}^{(0)} \circ F_i\, d\mu \tag{2.13}$$

[this follows from (1.9)]. We can write $\psi_{q_j}^{(0)} \circ F_i$ as an explicit linear combination of $\psi_{q_k}^{(0)}$ obtained from the minimizing property of $\mathcal{E}_1(\psi_{q_j}^{(0)})$. This gives a redundant set of three homogeneous linear equations. We also know

$$\sum_j \int \psi_{q_j}^{(0)}\, d\mu = 1 \tag{2.14}$$

because $\sum_j \psi_{q_j}^{(0)} \equiv 1$, and then we can solve for the integrals.

The second method we use is a fractal version of the finite element method (FEM) using piecewise harmonic splines. For the standard Laplacians this is described in detail in Gibbons *et al.*,[9] based on a discussion of spline spaces in Stricharz and Usher.[10] (These works also discuss piecewise biharmonic splines (the analog of cubic polynomial splines) that yield greater accuracy, but in the general context the difficulties involved in doing this are much greater.) The idea is to approximate functions on K by piecewise harmonic functions of level m, determined by values on V_m simply by

$$u = \sum_{x \in V_m} u(x) \psi_x^{(m)}. \tag{2.15}$$

Then $\mathcal{E}(u, \psi_x^{(m)}) = \mathcal{E}_m(u, \psi_x^{(m)})$ is still given by the right side of (2.2), but the left side is now

$$\int_K (\Delta u) \psi_x^{(m)}\, d\mu = \sum_{y \in V_m} \Delta u(y) \int_K \psi_y^{(m)} \psi_x^{(m)}\, d\mu. \tag{2.16}$$

We define the Gram matrix of level m

$$G_m(x,y) = \int_K \psi_y^{(m)} \psi_x^{(m)}\, d\mu. \tag{2.17}$$

Note that G is symmetric and sparse, since the product $\psi_y^{(m)} \psi_x^{(m)}$ is zero unless either $x = y$ or

$x \underset{m}{\sim} y$. So our FEM approximation to the eigenvalue problem is the generalized eigenvalue equation

$$-\sum_{x \underset{m}{\sim} y} c(x,y)\ (u(y)-u(x)) = \lambda \sum_{y} G_m(x,y)u(y). \tag{2.18}$$

(Note that it would be foolish to multiply by the inverse of the Gram matrix, even though it is invertible, because then we would obtain an eigenvalue equation for a matrix that is neither symmetric nor sparse.) To make this explicit we need to compute the Gram matrix.

If $x \underset{m}{\sim} y$ then $x = F_w q_j$ and $y = F_w q_k$ for $j \neq k$ and some word w with $|w| = m$. It is easy to see that the product $\psi_y^{(m)}\psi_x^{(m)}$ is supported in $F_w K$, and so

$$\begin{aligned} G_m(x,y) &= \int_{F_w K} \psi_y^{(m)}\psi_x^{(m)}\, d\mu \\ &= \mu_w \int \psi_{q_j}^{(0)}\psi_{q_k}^{(0)}\, d\mu. \end{aligned} \tag{2.19}$$

On the other hand, if $x = y \in V_m \backslash V_0$, then $x = F_w q_j = F_{w'} q_{j'}$ and $(\psi_x^{(m)})^2$ is supported on the union of the two cells $F_w K$ and $F_{w'} K$. Thus

$$\begin{aligned} G_m(x,x) &= \int_{F_w K} (\psi_x^{(m)})^2\, d\mu + \int_{F_{w'} K} (\psi_x^{(m)})^2\, d\mu \\ &= \mu_w \int_K (\psi_{q_j}^{(0)})^2\, d\mu + \mu_{w'} \int_K (\psi_{q_{j'}}^{(0)})^2\, d\mu. \end{aligned} \tag{2.20}$$

Finally, if $x = y = q_j$, then

$$G_m(q_j,q_j) = (\mu_j)^m \int \left(\psi_{q_j}^{(0)}\right)^2 d\mu \tag{2.21}$$

so we have reduced the computation to the case $m = 0$. Then we can use essentially the same method as we used to compute the integrals $\int \psi_{q_j}^{(0)}\, d\mu$. The analogy of (2.13) is

$$G_0(q_j,q_k) = \sum_i \mu_i \int (\psi_{q_j}^{(0)} \circ F_i)(\psi_{q_k}^{(0)} \circ F_i)\, d\mu \tag{2.22}$$

and we can express the right side of (2.22) as an explicit linear combination of entries of the Gram matrix. This gives us homogeneous linear equations for the entries, and we complete the story by using the inhomogeneous identity

$$\sum_j \sum_k G_0(q_j,q_k) = 1 \tag{2.23}$$

and solving.

We denote by $\tilde{u}_j^{(m)}$ and $\tilde{\lambda}_j^{(m)}$ the solutions to (2.18), with

$$0 = \tilde{\lambda}_0^{(m)} < \tilde{\lambda}_1^{(m)} \leq \cdots \leq \tilde{\lambda}_{N_m}^{(m)}. \tag{2.24}$$

We again have

$$\lambda_j = \lim_{m\to\infty} \tilde{\lambda}_j^{(m)}, \tag{2.25}$$

but this time the limit is decreasing. We get a good estimate of λ_j by averaging $\lambda_j^{(m)}$ and $\tilde{\lambda}_j^{(m)}$. Rather than a fair average, we use the estimate

$$\lambda_j \approx 0.625\lambda_j^{(m)} + 0.375\tilde{\lambda}_j^{(m)} \tag{2.26}$$

since this gives greater accuracy in the case of the standard Laplacian, where the exact values of the λ_j are known via spectral decimation.

The complete algorithms and computer code may be found on the website www.math.cornell.edu/~reu/twist. The actual computations use a variable depth level decomposition, rather than the uniform depth level described above, in order to increase accuracy.

In Table 1 we present the data for the values of $\lambda_j^{(m)}, \tilde{\lambda}_j^{(m)}$ and λ_j [via (2.26)] for three levels of approximation and $j \leq 40$, for the choice $(r_0, r_1, r_2) = (0.7267, 0.5281, 0.5281)$. This is the lattice case example with $(k_0, k_1, k_2) = (1, 2, 2)$. In Table 2 we present the data for $(r_0, r_1, r_2) = (0.7338, 0.6604, 0.3669)$, a non-lattice case. In Figs. 3 to 6 we display the graphs of $N(x)$ and $W(x)$ for these two Laplacians. Figures 7 to 10 show the same graphs for a selection of other Laplacians.

3. SELF-SIMILAR EMBEDDINGS AND OUTER APPROXIMATION

Fix a value of (ρ_0, ρ_1, ρ_2) on the surface (1.19), and let T be a triangle with vertices (q_0, q_1, q_2) and angles $(\alpha_0, \alpha_1, \alpha_2)$ such that $\rho_j = \cos\alpha_j$ (note that (1.19) guarantees $\alpha_0 + \alpha_1 + \alpha_2 = \pi$). Let $\{\tilde{F}_i\}$ be the IFS where $\tilde{F}_i$ fixes q_i, contracts by ρ_i and reflects about the angle bisector at q_i. The invariant set is a self-similar embedding of SG with twists in the plane. Figure 11 shows a selection of examples decomposed in m-cells for fixed m. Because these cells are of varying sizes, these are rather poor approximations of the fractals. In Fig. 12 we show the same examples decomposed into cells of varying levels but of approximately the same size (we choose a value of ϵ and decompose cells of diameter greater

Table 1 $(r_0, r_1, r_2) = (0.7267, 0.5281, 0.5281)$.

$\tilde{\lambda}_j{}^{(m)}$	$\lambda_j{}^{(m)}$	λ_j	$\tilde{\lambda}_j{}^{(m)}$	$\lambda_j{}^{(m)}$	λ_j	$\tilde{\lambda}_j{}^{(m)}$	$\lambda_j{}^{(m)}$	λ_j
0.0000	0.0000	0.0000	0.0000	0.0000	0.0000	0.0000	0.0000	0.0000
17.8800	17.8714	17.8746	17.8765	17.8734	17.8745	17.8752	17.8741	17.8745
28.2587	28.2372	28.2453	28.2499	28.2421	28.2450	28.2467	28.2439	28.2450
65.2279	65.1139	65.1566	65.1812	65.1395	65.1551	65.1642	65.1491	65.1548
115.6214	115.2560	115.3930	115.4746	115.3438	115.3928	115.4215	115.3741	115.3919
147.0196	146.4504	146.6638	146.7808	146.5703	146.6492	146.6952	146.6184	146.6472
181.2605	180.4047	180.7256	180.9004	180.5817	180.7012	180.7700	180.6534	180.6971
221.1196	219.7966	220.2927	220.5799	220.1025	220.2815	220.3869	220.2139	220.2788
265.2214	263.2893	264.0139	264.4486	263.7595	264.0179	264.1709	263.9222	264.0155
276.3321	274.2077	275.0043	275.4972	274.7465	275.0280	275.1952	274.9253	275.0265
359.5113	355.9336	357.2752	358.1030	356.8345	357.3102	357.5927	357.1367	357.3077
478.7636	473.1080	475.2288	476.2579	474.1026	474.9109	475.3554	474.5551	474.8552
499.1229	493.0505	495.3276	496.3990	494.0686	494.9425	495.4185	494.5501	494.8758
536.6801	529.7402	532.3427	533.5311	530.8525	531.8570	532.3984	531.3970	531.7725
686.7001	674.5743	679.1215	681.5785	677.1063	678.7834	679.7330	678.0943	678.7088
702.5382	689.8152	694.5864	697.1812	692.4969	694.2535	695.2504	693.5356	694.1787
806.6381	787.7354	794.8239	799.6767	793.1586	795.6029	797.1435	794.8537	795.7123
808.2782	789.7977	796.7279	801.2684	794.8080	797.2307	798.7239	796.4335	797.2924
919.9874	896.0437	905.0226	910.8672	902.4954	905.6348	907.5954	904.6335	905.7442
923.6215	899.5941	908.6044	914.4184	905.9999	909.1568	911.1221	908.1391	909.2577
1008.7511	980.3304	990.9882	997.8731	987.8752	991.6244	993.9360	990.3872	991.7180
1257.3699	1220.7875	1234.5059	1239.9151	1225.9427	1231.1824	1233.8532	1228.5685	1230.5502
1296.3910	1256.5853	1271.5124	1277.8063	1262.7760	1268.4124	1271.3906	1265.7557	1267.8688
1348.9044	1307.2377	1322.8627	1329.0511	1313.1263	1319.0981	1322.0443	1315.9985	1318.2657
1397.1953	1353.8571	1370.1090	1375.8198	1359.0483	1365.3376	1368.3032	1361.8686	1364.2815
1422.3259	1377.1216	1394.0732	1400.0745	1382.6418	1389.1791	1392.3139	1385.6439	1388.1452
1502.4179	1453.1245	1471.6095	1477.6566	1458.5028	1465.6855	1468.9847	1461.6011	1464.3699
1841.4054	1754.6837	1787.2043	1804.7431	1773.3331	1785.1118	1792.0376	1780.6548	1784.9234
1850.9681	1764.3894	1796.8564	1813.8533	1782.3523	1794.1652	1801.0101	1789.5466	1793.8454
1929.5883	1838.3841	1872.5857	1889.7961	1856.3779	1868.9097	1875.7082	1863.3939	1868.0118
1941.4494	1851.0859	1884.9722	1900.9815	1867.6137	1880.1266	1886.7125	1874.3218	1878.9683
1975.4023	1879.7035	1915.5905	1933.7700	1898.6969	1911.8494	1919.0249	1906.1217	1910.9604
2129.4149	2004.9353	2051.6151	2082.0583	2037.7987	2054.3961	2065.2259	2049.6973	2055.5205
2130.0107	2005.7800	2052.3665	2082.6036	2038.3901	2054.9702	2065.7591	2050.2332	2056.0554
2270.9767	2122.6787	2178.2905	2218.9891	2166.7101	2186.3147	2199.8601	2181.8863	2188.6265
2273.0940	2126.5859	2181.5264	2220.7568	2168.9462	2188.3752	2201.5753	2183.6654	2190.3816
2276.5298	2133.0709	2186.8680	2223.6189	2172.5861	2191.7234	2204.3517	2186.5477	2193.2242
2280.0523	2139.3316	2192.1019	2226.5704	2176.2883	2195.1441	2207.2162	2189.5151	2196.1531
2750.6012	2549.7860	2625.0917	2673.5840	2600.9057	2628.1601	2645.8315	2620.2812	2629.8626
2783.0586	2577.7112	2654.7165	2704.2257	2629.8873	2657.7642	2675.8475	2649.7132	2659.5136
2843.0336	2629.2279	2709.4051	2760.8223	2683.3014	2712.3717	2731.2711	2704.0257	2714.2427

than ϵ). We will use these types of approximations. In Fig. 13 we show a sequence of decompositions for a single fractal with varying diameter size.

We write such a cell decomposition

$$K = \bigcup_{w \in \mathcal{P}} F_w K \tag{3.1}$$

where $\mathcal{P}$ is the approximate set of words, called a *partition*. A natural choice of approximating domains would be $\Omega' = \bigcup_{w \in \mathcal{P}} F_w T^0$, where T^0 denotes the interior of the triangle, but these domains are not connected. We need a slight modification to obtain connectivity. In Berry *et al.*,[4] the triangle T was enlarged slightly, but we found a method that yields much greater accuracy in the case $(\rho_0, \rho_1, \rho_2) = (\frac{1}{2}, \frac{1}{2}, \frac{1}{2})$ (the equilateral triangle case), and in all cases appear to converge rapidly. The idea is that we view the domain Ω'

Table 2 $(r_0, r_1, r_2) = (0.7338, 0.6604, 0.3669)$.

$\tilde{\lambda}_j{}^{(m)}$	$\lambda_j{}^{(m)}$	λ_j	$\tilde{\lambda}_j{}^{(m)}$	$\lambda_j{}^{(m)}$	λ_j	$\tilde{\lambda}_j{}^{(m)}$	$\lambda_j{}^{(m)}$	λ_j
0.0000	0.0000	0.0000	0.0000	0.0000	0.0000	0.0000	0.0000	0.0000
16.3804	16.3793	16.3797	16.3818	16.3785	16.3798	16.3839	16.3768	16.3795
35.5030	35.4978	35.4997	35.5095	35.4946	35.5002	35.5247	35.4920	35.5043
65.2675	65.2493	65.2561	65.2881	65.2359	65.2555	65.3342	65.2221	65.2641
90.2505	90.2161	90.2290	90.2908	90.1936	90.2300	90.3904	90.1730	90.2545
132.4827	132.4073	132.4356	132.5724	132.3671	132.4441	132.7838	132.3382	132.5053
177.5597	177.4208	177.4729	177.7201	177.3638	177.4974	178.0187	177.2258	177.5231
220.7979	220.5859	220.6654	221.0348	220.4920	220.6955	221.6204	220.3627	220.8343
281.8900	281.5532	281.6795	282.2442	281.3656	281.6951	283.2622	281.2348	281.9950
306.6400	306.2239	306.3799	307.1151	305.9501	306.3870	308.2206	305.6620	306.6215
357.9062	357.3631	357.5667	358.5884	357.1628	357.6974	360.0949	356.7671	358.0150
426.7751	426.0185	426.3023	427.7322	425.6633	426.4391	429.5689	424.5419	426.4270
500.1202	499.0765	499.4679	501.3565	498.4569	499.5442	503.4926	496.7290	499.2653
552.0122	550.7229	551.2064	553.5409	549.9789	551.3147	556.3789	547.9929	551.1376
605.3365	603.8243	604.3914	607.0356	602.6262	604.2797	610.8727	600.9435	604.6669
641.5373	639.7384	640.4130	643.6870	638.4444	640.4104	647.6073	635.6317	640.1225
756.3415	753.9129	754.8236	759.1844	752.4937	755.0027	766.0254	750.6742	756.4309
843.3138	840.5031	841.5571	846.4076	838.7120	841.5978	854.2820	834.9364	842.1910
863.0294	859.6930	860.9441	866.8643	857.2380	860.8479	875.2884	853.9541	861.9544
878.5461	875.4711	876.6242	882.1249	874.1189	877.1212	889.9780	869.9759	877.4767
990.9869	986.8295	988.3885	996.2592	984.7015	989.0356	1006.1707	979.4493	989.4698
1096.0205	1090.9141	1092.8290	1100.8193	1085.9383	1091.5187	1114.6116	1080.5568	1093.3274
1111.6527	1106.2101	1108.2511	1117.6027	1101.7473	1107.6931	1130.7913	1098.7809	1110.7848
1235.4963	1229.2180	1231.5724	1242.4609	1223.8202	1230.8104	1258.6365	1212.6836	1229.9159
1256.4263	1249.4473	1252.0644	1263.8498	1242.6374	1250.5920	1280.8782	1237.4449	1253.7324
1380.4791	1372.3928	1375.4252	1389.3408	1366.3397	1374.9651	1407.8261	1355.9379	1375.3960
1411.9799	1403.1063	1406.4339	1421.8980	1396.8325	1406.2320	1446.8633	1390.4549	1411.6080
1523.5362	1513.4596	1517.2383	1534.2922	1501.8572	1514.0203	1559.9651	1501.7996	1523.6117
1657.2989	1645.2975	1649.7980	1669.5041	1632.8941	1646.6229	1704.3776	1633.6382	1660.1655
1665.0351	1653.5189	1657.8375	1678.0810	1644.8105	1657.2869	1712.5745	1640.9691	1667.8211
1762.1746	1747.6708	1753.1098	1778.0023	1733.4075	1750.1305	1812.9998	1729.7285	1760.9553
1848.6627	1834.4040	1839.7510	1865.0790	1825.3714	1840.2617	1895.7809	1807.1852	1840.4086
2095.7995	2077.6256	2084.4408	2116.1659	2060.2428	2081.2139	2175.8912	2061.4757	2104.3815
2128.4786	2109.9667	2116.9087	2147.7975	2094.8389	2114.6984	2200.8704	2081.1648	2126.0544
2203.7062	2184.5137	2191.7109	2225.4533	2163.9479	2187.0124	2284.4387	2150.9213	2200.9903
2323.4719	2302.4326	2310.3223	2347.5030	2289.0945	2310.9977	2419.2436	2290.9668	2339.0706
2365.3176	2338.8206	2348.7570	2395.9989	2323.3185	2350.5737	2469.8033	2317.2230	2374.4406
2382.1086	2360.6403	2368.6909	2406.3171	2343.3888	2366.9869	2480.0067	2338.7577	2391.7261
2407.5911	2385.4914	2393.7788	2434.4478	2369.7882	2394.0355	2500.6108	2359.1340	2412.1878
2484.4108	2459.2506	2468.6857	2511.3782	2434.7877	2463.5091	2585.6470	2404.3356	2472.3274
2654.2548	2622.9905	2634.7146	2689.0682	2595.4934	2630.5840	2772.8002	2575.7586	2649.6492

subtractively, as T^0 with some closed triangles removed, $\Omega' = T^0 \backslash \cup T_j$. We then clip off little neighborhoods of the vertices of each T_j to get $T_j' \subset T_j$, and take $\Omega = T^0 \backslash \cup T_j'$. The clipped-off neighborhoods create little passages that make Ω connected. To do this in a uniform fashion we choose a small parameter δ, and near a vertex of T_j with angle θ we inscribe a circle of radius $\delta \tan \theta/2$ (so the distance from the circle to the vertex along the edges is δ), and we remove the region between the circle and the vertex. We choose δ to be constant over all triangles T_j, but it will vary with the approximation. This is illustrated in Fig. 14 that shows the standard gasket with the inscribed circles and

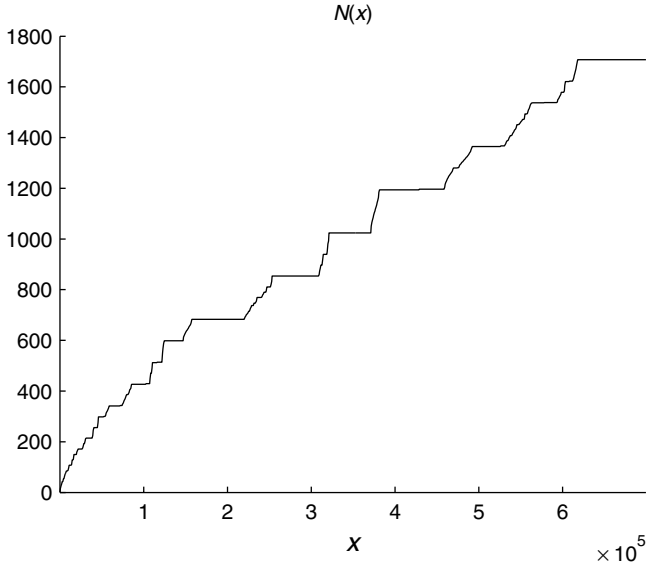

Fig. 3 The graph of $N(x)$ for $(r_0, r_1, r_2) = (0.7267, 0.5281, 0.5281)$.

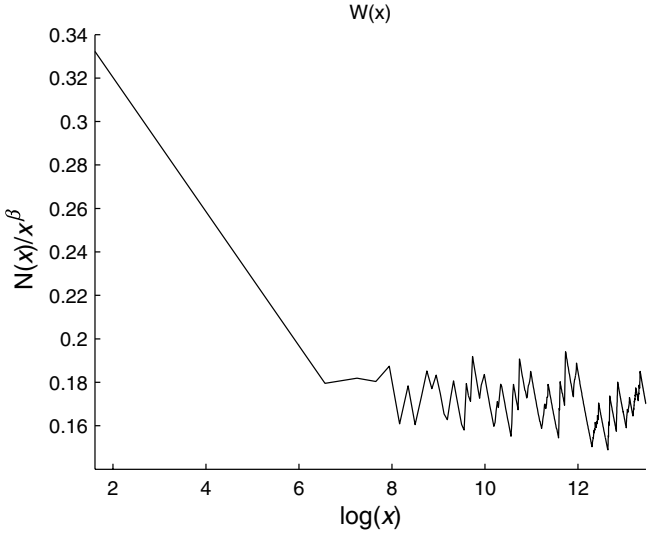

Fig. 4 The graph of $W(x)$ versus $\log x$ for $(r_0, r_1, r_2) = (0.7267, 0.5281, 0.5281)$.

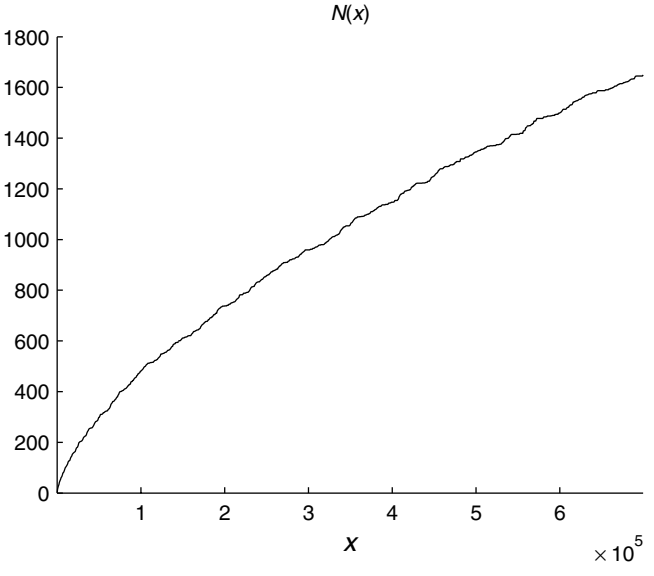

Fig. 5 The graph of $N(x)$ for $(r_0, r_1, r_2) = (0.7338, 0.6604, 0.3669)$.

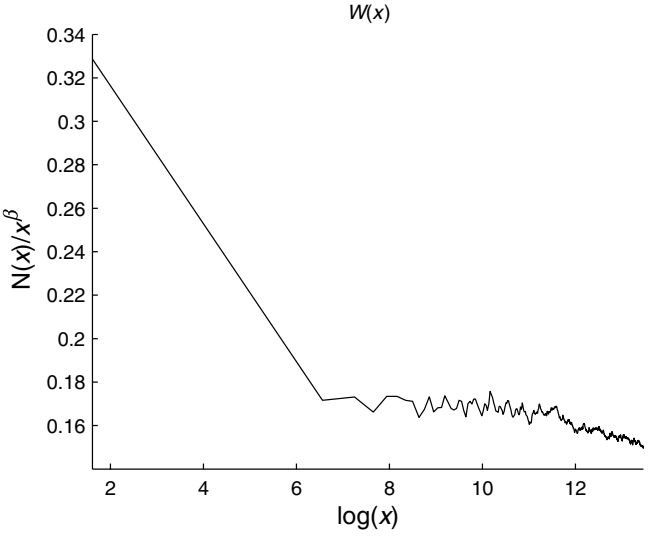

Fig. 6 The graph of $W(x)$ versus $\log x$ for $(r_0, r_1, r_2) = (0.7338, 0.6604, 0.3669)$.

Fig. 15 that shows the approximation of the standard gasket. (For the actual Matlab FEM routine we use polygonal approximations to the circle arcs.)

We choose a decreasing sequence $\{\epsilon_n\}$ of maximum diameter cut-offs and a corresponding sequence $\{\delta_n\}$ to yield a sequence of connected domains Ω_n. Let

$$0 = \overline{\lambda}_0^{(n)} < \overline{\lambda}_1^{(n)} \leq \cdots \tag{3.2}$$

denote the eigenvalues of the Neumann Laplacian on Ω_n, with corresponding eigenfunctions

$$-\Delta \overline{u}_j^{(n)} = \overline{\lambda}_j^{(n)} \overline{u}_j^{(n)}. \tag{3.3}$$

The premise of the method of outer approximation is that there exist appropriate renormalization factors s_n such that $s_n \overline{\lambda}_j^{(n)}$ converges as $n \to \infty$ for each j, and the eigenfunctions $\overline{u}_j^{(n)}$ restricted to K also converge (again after proper normalization). Our numerical data supports this premise. If the Ω_n are chosen appropriately, it may be true that we can take $s_n = s^n$ for some s, but we do not have enough data to support this idea. In the standard case, the renormalization factors tend to infinity, but in other cases they tend to zero. (This is based on data for small values of j.) Presumably there will

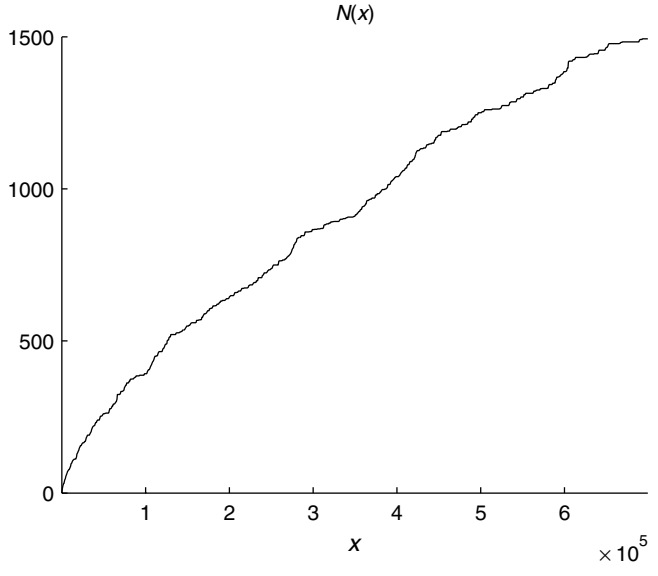

Fig. 7 The graph of $N(x)$ for $(r_0, r_1, r_2) = (0.6652, 0.5654, 0.5654)$.

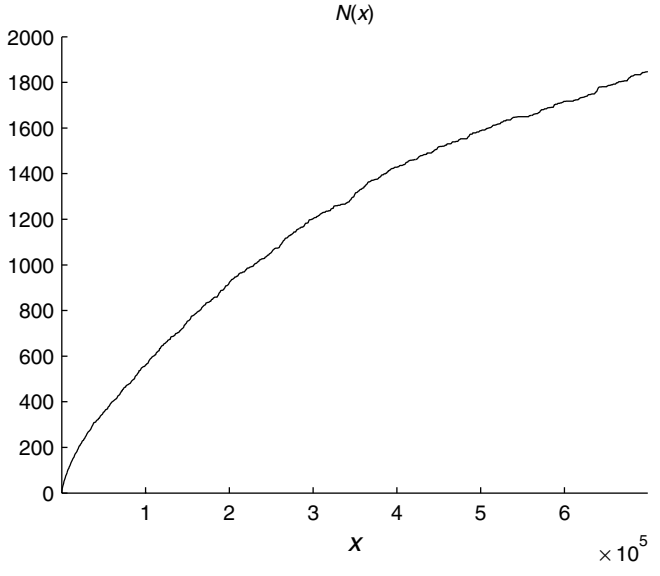

Fig. 9 The graph of $N(x)$ for $(r_0, r_1, r_2) = (1, 0.4, 0.65)$.

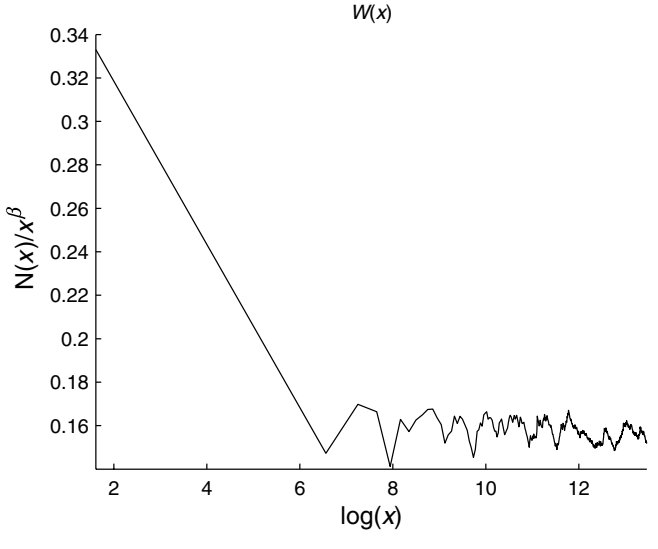

Fig. 8 The graph of $W(x)$ versus $\log x$ for $(r_0, r_1, r_2) = (0.6652, 0.5654, 0.5654)$.

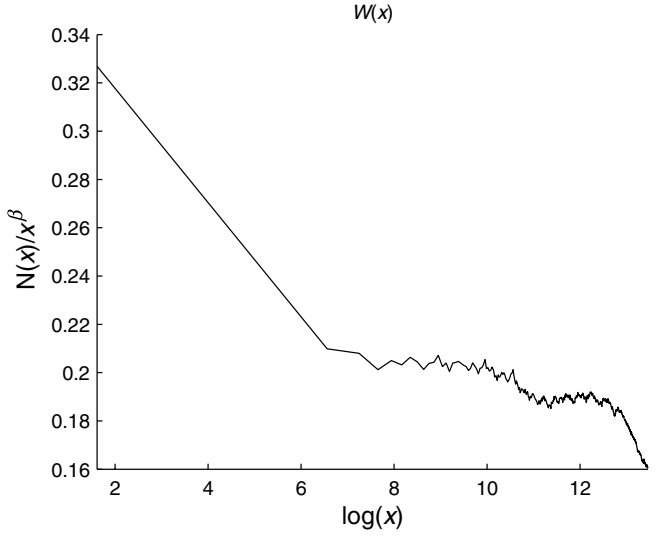

Fig. 10 The graph of $W(x)$ versus $\log x$ for $(r_0, r_1, r_2) = (0.8371, 0.5441, 0.3348)$.

be some values of (ρ_0, ρ_1, ρ_2) where we can take all $s_n = 1$, but our data is not accurate enough to pin down such values.

To avoid dealing with the renormalization factors, we renormalize all spectra by computing the values $\overline{\lambda}_j^{(n)}/\overline{\lambda}_1^{(n)}$, so the first renormalized eigenvalue is always 1. In Tables 3 and 4 we present these values for these successive Ω_n for two different choices of (ρ_0, ρ_1, ρ_2). The first is a lattice case example with $(k_0, k_1, k_2) = (1, 2, 2)$, and the second is a non-lattice case. The data is obtained by using the Matlab FEM solver, which automatically triangulates the region and uses piecewise linear splines. One such triangulation is shown in Fig. 16.

Matlab is also able to refine the chosen triangulation to increase accuracy, at the expense of greater running time. Note that this FEM is not the same as the FEM used in Sec. 2, but it also has the property that it approximates from above.

Tables 5 and 6 report the ratios $\overline{\lambda}_j^{(n+1)}/\overline{\lambda}_j^{(n)}$ for the unnormalized eigenvalue approximations for the two examples. More data may be found on the website www.math.cornell.edu/~reu/twist.

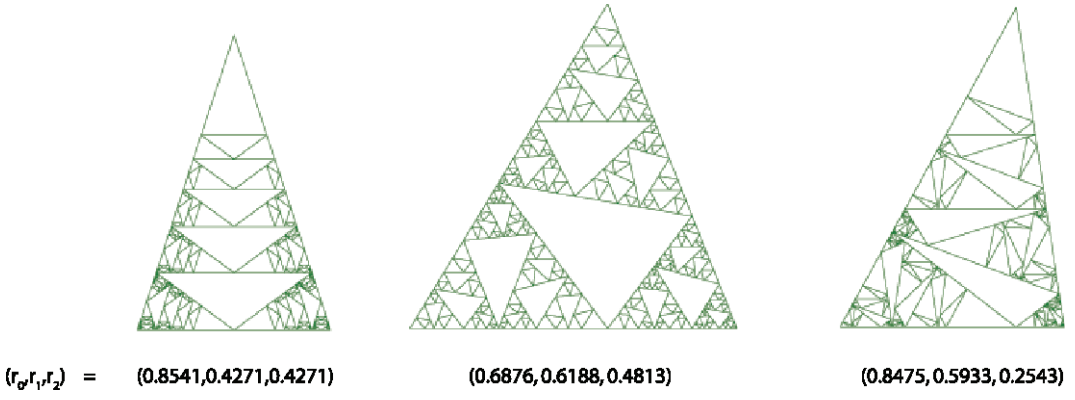

Fig. 11 SG decomposed in m-cells for fixed $m = 6$.

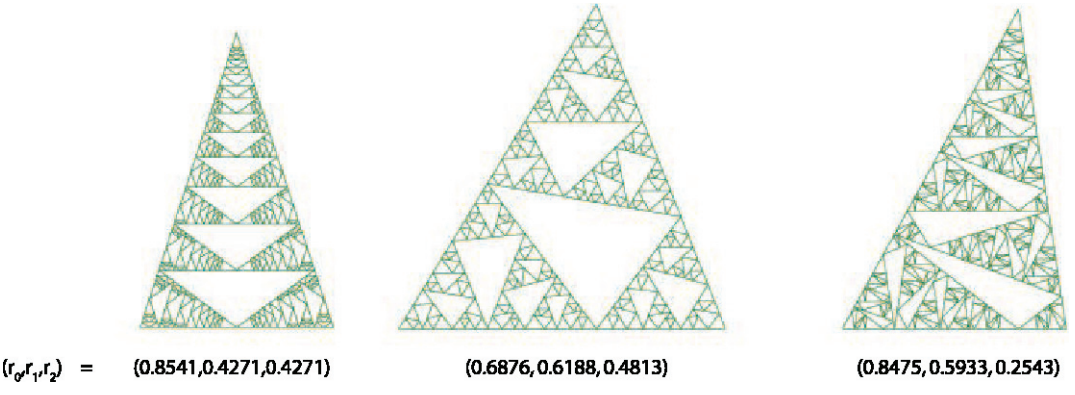

Fig. 12 SG decomposed into cells of approximately the same size.

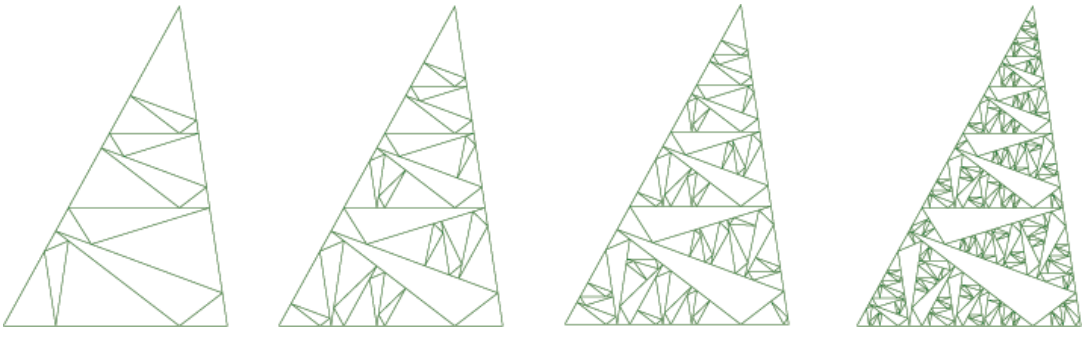

Fig. 13 A sequence of decompositions for a single fractal with varying diameter size.

4. COMPARISON OF SPECTRA

In order to compare spectra from the fractal Laplacian and the outer approximation method, we renormalize all spectra by dividing by the first nonzero eigenvalue. We already did this in Sec. 3. In Sec. 2 we reported unnormalized eigenvalues, since the Laplacian has an exact spectrum. However, the energy is only characterized up to a constant multiple, so it is not clear that the particular choice of initial conductances $\{c_{jk}\}$ that we used are in any way natural or canonical. For that reason we are not really losing any significant information when we renormalize the spectrum. In all cases we start with parameters (r_0, r_1, r_2) for the fractal Laplacian and compute the corresponding parameters (ρ_0, ρ_1, ρ_2) via (1.20) and (1.21).

In Table 7 we give the best approximation of an initial segment of the two spectra for the standard Laplacian $(r_0, r_1, r_2) = (\frac{3}{5}, \frac{3}{5}, \frac{3}{5})$ and $(\rho_0, \rho_1, \rho_2) = (\frac{1}{2}, \frac{1}{2}, \frac{1}{2})$. The same data is shown

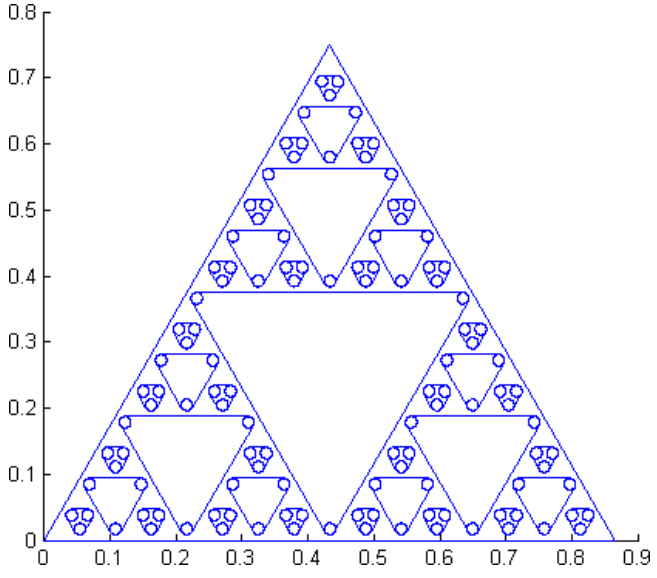

Fig. 14 The standard gasket with inscribed circles.

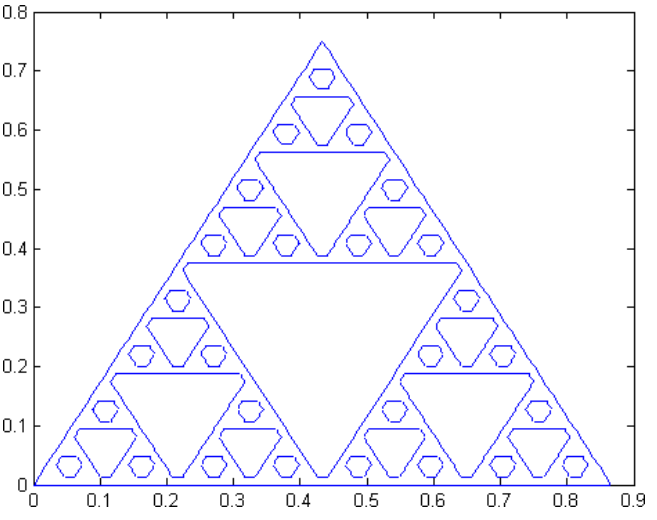

Fig. 15 Outer approximation of the standard gasket.

graphically in Fig. 17. Note that even when the numerical values differ noticeably, there is still a qualitative similarity in the graphs. The numerical agreement here is much stronger than the results in Berry *et al.*,[4] which used a different sequence of approximating domains.

In Tables 8 and 9 and Figs. 18 and 19 we give the same data for two more lattice cases. In Tables 10 and 11 and the corresponding Figs. 20

Table 3 Outer approximation for Successive Ω_n for Lattice Case with $(k_0, k_1, k_2) = (1, 2, 2)$ Using the Third Mesh Refinement.

k	$\overline{\lambda}_k^{(1)}$ for $\epsilon_1 = 0.1$	$\overline{\lambda}_k^{(2)}$ for $\epsilon_2 = 0.05$	$\overline{\lambda}_k^{(3)}$ for $\epsilon_3 = 0.025$	k	$\overline{\lambda}_k^{(1)}$ for $\epsilon_1 = 0.1$	$\overline{\lambda}_k^{(2)}$ for $\epsilon_2 = 0.05$	$\overline{\lambda}_k^{(3)}$ for $\epsilon_3 = 0.025$
2	3.0054	3.0036	3.1016	27	230.1850	244.0057	253.8197
3	4.8254	4.7911	4.9374	28	271.2435	298.7589	310.9698
4	10.8394	10.9002	11.3142	29	273.0022	300.3190	312.5188
5	19.8155	19.6045	20.1156	30	288.8534	311.1107	325.3433
6	24.2714	24.5793	25.5962	31	291.1689	312.6618	326.9210
7	29.7269	30.0137	31.3957	32	293.3271	318.3030	332.2885
8	37.1844	37.3817	38.5511	33	297.1452	347.8540	359.3666
9	44.4833	44.6698	45.9081	34	297.5306	347.9483	359.8783
10	46.6469	46.6344	47.8094	35	305.1095	366.0712	380.6041
11	60.1017	60.5395	62.2619	36	306.7676	366.5043	380.6949
12	79.0952	78.4946	82.5405	37	310.9881	367.1052	381.5178
13	82.3826	81.6028	85.9900	38	312.5521	367.1295	381.9275
14	88.4365	87.6016	92.4321	39	362.6193	437.4344	457.4669
15	112.9808	113.1100	118.1953	40	365.5773	442.0996	462.6731
16	115.8304	115.8378	120.9950	41	371.1921	451.8689	472.8840
17	133.8250	133.7415	138.3605	42	374.0436	457.9557	479.9252
18	134.6725	134.5194	138.9148	43	377.7701	465.0813	487.4827
19	150.8885	152.4357	157.8633	44	699.7585	561.9619	616.4579
20	151.5526	153.2330	158.8763	45	706.3876	571.4931	627.2202
21	165.4861	166.0872	173.0456	46	715.4798	578.6869	634.3195
22	193.8871	205.3829	213.6537	47	715.8576	579.4500	636.9564
23	200.3061	211.7301	220.1937	48	741.1138	594.7465	651.7928
24	206.5024	219.8432	228.7570	49	743.5864	596.2774	653.8485
25	214.0529	227.6267	236.7381	50	745.7984	616.4991	675.9083
26	218.2697	231.8121	240.9795				

Table 4 Outer Approximation for Successive Ω_n for Non-Lattice Case with $(r_0, r_1, r_2) = (0.6407, 0.6407, 0.5126)$.

k	$\overline{\lambda}_k^{(1)}$ for $\epsilon_1 = 0.1$	$\overline{\lambda}_k^{(2)}$ for $\epsilon_2 = 0.05$	$\overline{\lambda}_k^{(3)}$ for $\epsilon_3 = 0.025$	k	$\overline{\lambda}_k^{(1)}$ for $\epsilon_1 = 0.1$	$\overline{\lambda}_k^{(2)}$ for $\epsilon_2 = 0.05$	$\overline{\lambda}_k^{(3)}$ for $\epsilon_3 = 0.025$
2	3.3412	3.2772	3.4351	27	257.6586	258.436	291.2836
3	4.4268	4.4799	4.6754	28	279.2622	288.9922	329.7366
4	14.4917	15.7453	16.3976	29	290.7262	302.8475	342.196
5	15.3958	16.2011	16.9859	30	295.8093	306.9612	347.2723
6	21.1689	21.4397	22.3647	31	308.2649	317.3786	358.1169
7	35.4676	33.0958	34.6485	32	309.9739	327.6054	358.8984
8	40.9223	42.1461	44.2842	33	311.4715	334.0112	367.5322
9	46.3538	43.3581	44.7699	34	318.4612	336.2633	369.8387
10	59.6418	61.0546	67.2832	35	326.6663	363.5218	374.807
11	62.1507	62.3431	68.1003	36	327.9416	365.2178	375.0562
12	72.6398	75.4552	82.8393	37	331.0148	370.4838	380.981
13	80.514	80.6803	86.1174	38	344.8075	401.1682	418.9393
14	89.362	86.9142	91.2267	39	345.5013	402.2135	419.5983
15	98.6675	96.0501	101.3358	40	566.7065	549.9809	562.3849
16	134.3273	143.1652	143.0577	41	569.0164	550.8086	564.1144
17	135.0787	144.2425	144.1883	42	574.3514	555.8709	569.6954
18	157.4237	165.2669	167.8939	43	575.881	557.001	571.6285
19	161.2369	168.6998	178.4038	44	593.7856	637.7689	647.654
20	164.7817	170.4516	180.0923	45	599.0171	640.4132	656.0964
21	173.8276	186.1656	184.3523	46	601.365	647.4029	662.7673
22	175.1665	189.2562	185.7811	47	605.6756	649.8289	669.0267
23	178.0961	193.2652	186.5998	48	621.4816	664.8719	705.3707
24	245.5395	246.1592	281.7031	49	624.2777	670.5822	713.2526
25	249.2688	250.8471	282.6705	50	630.5624	675.9373	721.2077
26	251.9542	253.5524	287.2007				

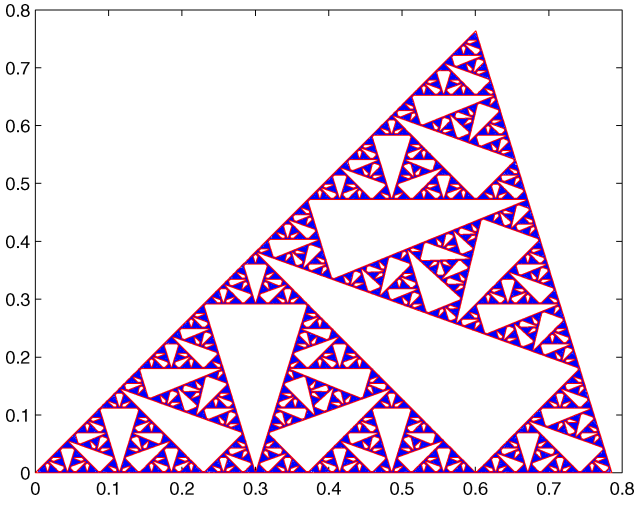

Fig. 16 A triangulation.

and 21 we give the same data for two non-lattice cases. We see differences of no more than 2% for close to 100 eigenvalue, with most differences much smaller. More data may be found on the website www.math.cornell.edu/˜reu/twist.

5. FEATURES OF THE SPECTRA

The spectrum of the standard Laplacian is quite striking, featuring both high multiplicities and large gaps. The high multiplicities, associated with the existence of localized eigenfunctions, may be explained in two ways, either by spectral decimation Fukushima and Shima,[11] or by the existence of a nonabelian symmetry group Barlow and Kigami.[12] Spectral decimation also explains large gaps. See Adams *et al.*[13] for numerical approximations to the spectrum of the standard Laplacian on the pentagasket. This is an example where spectral decimation is known to fail Shima,[14] but there is a dihedral-5 symmetry group. The data shows both high multiplicities and large spectral gaps, but as yet there is no proof of the existence of the gaps.

Neither feature is possible in the non-lattice case[7] because the Weyl ratio has a limit. We do not see evidence of multiplicities greater than 1 in any of the lattice cases. We see some evidence of large spectral gaps, but they are not large enough to be convincing. The precise question here is whether

Table 5 Ratios $\overline{\lambda}_j^{(n+1)}/\overline{\lambda}_j^{(n)}$ of the Unnormalized Eigenvalue Approximations from the Outer Approximation Method with the Second Mesh Refinement for Lattice Case with $(k_0, k_1, k_2) = (1, 2, 2)$.

k	$\overline{\lambda}_k^{(2)}/\overline{\lambda}_k^{(1)}$	$\overline{\lambda}_k^{(3)}/\overline{\lambda}_k^{(2)}$	k	$\overline{\lambda}_k^{(2)}/\overline{\lambda}_k^{(1)}$	$\overline{\lambda}_k^{(3)}/\overline{\lambda}_k^{(2)}$	k	$\overline{\lambda}_k^{(2)}/\overline{\lambda}_k^{(1)}$	$\overline{\lambda}_k^{(3)}/\overline{\lambda}_k^{(2)}$
2	1	1.03	19	1.01	1.04	36	1.19	1.04
3	0.99	1.03	20	1.01	1.04	37	1.18	1.04
4	1.01	1.04	21	1	1.04	38	1.17	1.04
5	0.99	1.03	22	1.06	1.04	39	1.21	1.05
6	1.01	1.04	23	1.06	1.04	40	1.21	1.05
7	1.01	1.05	24	1.06	1.04	41	1.22	1.0
8	1.01	1.03	25	1.06	1.04	42	1.22	1.0
9	1	1.03	26	1.06	1.04	43	1.23	1.0
10	1	1.03	27	1.06	1.04	44	0.8	1.1
11	1.01	1.03	28	1.1	1.04	45	0.81	1.1
12	0.99	1.05	29	1.1	1.04	46	0.81	1.1
13	0.99	1.05	30	1.08	1.05	47	0.81	1.1
14	0.99	1.06	31	1.07	1.05	48	0.8	1.1
15	1	1.05	32	1.09	1.04	49	0.8	1.1
16	1	1.04	33	1.17	1.03	50	0.83	1.1
17	1	1.03	34	1.17	1.03			
18	1	1.03	35	1.2	1.04			

Table 6 Ratios $\overline{\lambda}_j^{(n+1)}/\overline{\lambda}_j^{(n)}$ of the Unnormalized Eigenvalue Approximations from the Outer Approximation Method with the Zero Mesh Refinement for Non-Lattice Case with $(r_0, r_1, r_2) = (0.6407, 0.6407, 0.5126)$.

k	$\overline{\lambda}_k^{(2)}/\overline{\lambda}_k^{(1)}$	$\overline{\lambda}_k^{(3)}/\overline{\lambda}_k^{(2)}$	k	$\overline{\lambda}_k^{(2)}/\overline{\lambda}_k^{(1)}$	$\overline{\lambda}_k^{(3)}/\overline{\lambda}_k^{(2)}$	k	$\overline{\lambda}_k^{(2)}/\overline{\lambda}_k^{(1)}$	$\overline{\lambda}_k^{(3)}/\overline{\lambda}_k^{(2)}$
2	0.98	1.05	19	1.05	1.06	36	1.11	1.03
3	1.01	1.04	20	1.03	1.06	37	1.12	1.03
4	1.09	1.04	21	1.07	0.99	38	1.16	1.04
5	1.05	1.05	22	1.08	0.98	39	1.16	1.04
6	1.01	1.04	23	1.09	0.97	40	0.97	1.02
7	0.93	1.05	24	1	1.14	41	0.97	1.02
8	1.03	1.05	25	1.01	1.13	42	0.97	1.02
9	0.94	1.03	26	1.01	1.13	43	0.97	1.03
10	1.02	1.1	27	1	1.13	44	1.07	1.02
11	1	1.09	28	1.03	1.14	45	1.07	1.02
12	1.04	1.1	29	1.04	1.13	46	1.08	1.02
13	1	1.07	30	1.04	1.13	47	1.07	1.03
14	0.97	1.05	31	1.03	1.13	48	1.07	1.06
15	0.97	1.06	32	1.06	1.1	49	1.07	1.06
16	1.07	1	33	1.07	1.1	50	1.07	1.07
17	1.07	1	34	1.06	1.1			
18	1.05	1.02	35	1.11	1.03			

there exists a constant $s > 0$ such that

$$\frac{\lambda_{j+1} - \lambda_j}{\lambda_j} \geq s \quad \text{for infinitely many } j. \tag{5.1}$$

For the standard Laplacian this is valid for a value of $s > 1$. We see many gaps with a value around $s = 0.1$, but gaps of this size also show up in some non-lattice cases. Indeed, it is difficult to distinguish between the two cases from our data. Of course, both lattice and non-lattice cases are dense in the set of parameters, but the point is that only lattice cases with relatively small values of $\{k_i\}$ should be distinguishable with the precision level of computation we must accept, and these are few and far between.

Table 7 Comparison of Normalized Eigenvalues for the Outer Approximation and FEM methods. Standard Case with $(r_0, r_1, r_2) = (\frac{3}{5}, \frac{3}{5}, \frac{3}{5})$.

k	$\overline{\lambda}_k$	λ_k	k	$\overline{\lambda}_k$	λ_k	k	$\overline{\lambda}_k$	λ_k
2	1.0000	1.0000	19	40.5196	40.4470	36	125.0003	124.7427
3	1.0000	1.0045	20	40.5196	40.5237	37	125.0003	124.8172
4	5.0000	4.9977	21	40.5196	40.6524	38	125.0003	124.8330
5	5.0000	5.0023	22	49.0160	48.9594	39	125.0003	124.9187
6	5.0000	5.0226	23	49.0160	49.0677	40	125.0003	124.9887
7	8.1039	8.0993	24	51.5278	51.4582	41	125.0003	125.2686
8	8.1039	8.1309	25	51.5278	51.5372	42	125.0003	125.3296
9	10.3056	10.3160	26	51.5278	51.5621	43	158.9238	158.3860
10	25.0000	24.9481	27	51.5278	51.6117	44	158.9238	158.4357
11	25.0000	24.9571	28	125.0003	124.3883	45	158.9238	158.5192
12	25.0000	24.9661	29	125.0003	124.4808	46	158.9238	158.6953
13	25.0000	25.0045	30	125.0003	124.4808	47	162.6063	162.1174
14	25.0000	25.0248	31	125.0003	124.5440	48	162.6063	162.1693
15	25.0000	25.1061	32	125.0003	124.6095	49	175.6999	174.9481
16	31.7847	31.7878	33	125.0003	124.6479	50	175.6999	175.1490
17	35.1398	35.0813	34	125.0003	124.6749			
18	35.1398	35.2054	35	125.0003	124.6862			

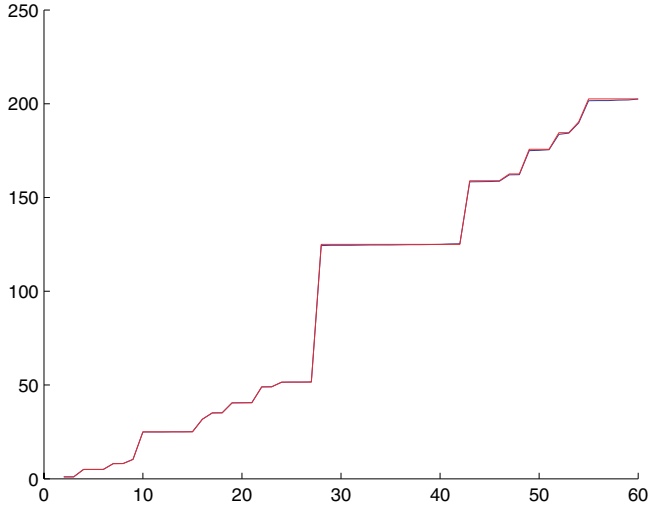

Fig. 17 Comparison of normalized eigenvalues for the outer approximation and FEM methods. Standard case with $(r_0, r_1, r_2) = (\frac{3}{5}, \frac{3}{5}, \frac{3}{5})$.

The existence of spectral gaps is significant, since they imply (in the presence of sub-Gaussian heat kernel estimates[1]) the uniform convergence of eigenfunction expansions of continuous functions when the partial sums are taken up to a gap.[15] It is somewhat disappointing that we cannot offer experimental evidence for the existence of gaps. On the other hand, the experimental evidence does not suggest that they do not exist.

Despite the absence of multiplicities greater than 1 in the spectra, there is an intriguing feature of clustering of eigenvalues, meaning that there are many eigenvalues that are nearly equal. This occurs in both lattice and non-lattice cases, although the existence of a limit for the Weyl ratio in the non-lattice case limits the cluster sizes. This clustering also occurs in spectra of other fractal Laplacians[4,16] but does not seem to occur in non-fractal cases.[17–19] (Of course there is a different type of clustering that occurs when you perturb a Laplacian which has high multiplicity eigenvalues. See Weinstein[20] and Guillemin[21] for the sphere, and Okoudjou and Strichartz[22] for SG.)

Sometimes, the eigenvalues in a cluster are so close that one might be tempted to conjecture that they are identical, but we do not believe this is the case. Some of the reasons are the sporadic nature of these coincidences, that they do not occur lower in the spectrum, and that they occur for just two eigenvalues in a large cluster. Moreover, there is no apparent relationship between the associated eigenfunctions.

For all our Laplacians, the power growth rate x^β for $N(x)$ given by (1.15) has $\beta < 1$ (this follows since $\sum \mu_i = 1$ and $r_i < 1$, so $\sum r_i \mu_i < 1$). This means that $\lambda_j \approx j^{1/\beta}$, so the average value of $\lambda_{j+1} - \lambda_j$ goes to infinity. Something very special must be going on to make eigenvalues cluster together. This deserves investigation.

We have also looked at the possibility of miniaturization of eigenfunctions, where an eigenfunction of higher eigenvalue is built out of eigenfunctions

Table 8 Comparison of Normalized Eigenvalues for the Outer Approximation and FEM Methods. Lattice Case with $(k_0, k_1, k_2) = (1, 1, 2)$.

k	$\overline{\lambda}_k$	λ_k	k	$\overline{\lambda}_k$	λ_k	k	$\overline{\lambda}_k$	λ_k
2	1	1	19	54.78	55.61	36	154.01	151.4
3	1.69	1.7	20	58.04	58.8	37	157.2	154.58
4	4.35	4.4	21	59.58	60.26	38	158.18	155.48
5	4.84	4.88	22	64.07	64.66	39	161.13	158.91
6	7.2	7.24	23	65.28	65.81	40	164.19	161.99
7	11.67	11.63	24	67.99	68.65	41	170.64	169.04
8	15.31	15.28	25	73.45	74.44	42	202.53	200.01
9	16.42	16.4	26	82.3	83.42	43	202.95	200.49
10	18.3	18.35	27	85.4	86.62	44	203.53	201.07
11	19.04	19.07	28	91.27	92.53	45	204.48	202.29
12	25.46	25.39	29	91.53	92.79	46	208.86	207.02
13	25.72	25.81	30	92.52	93.37	47	214.85	212.67
14	27.57	27.63	31	95.2	95.97	48	217.62	215.82
15	29.43	29.51	32	96.97	97.6	49	219.15	217.14
16	42.08	43.02	33	100.85	101.77	50	227.47	226.18
17	42.41	43.05	34	105.16	106.71			
18	54.51	55.43	35	105.67	106.8			

Table 9 Comparison of Normalized Eigenvalues for the Outer Approximation and FEM Methods. Lattice Case with $(k_0, k_1, k_2) = (1, 3, 3)$.

k	$\overline{\lambda}_k$	λ_k	k	$\overline{\lambda}_k$	λ_k	k	$\overline{\lambda}_k$	λ_k
2	1	1	19	55.83	55.45	36	155.74	157.02
3	2.07	2.05	20	62.95	62.35	37	155.97	157.05
4	3.37	3.37	21	70.51	70.08	38	156.1	157.14
5	7.19	7.15	22	73.65	72.88	39	162.01	161.19
6	7.43	7.45	23	74.43	74.71	40	163.29	161.21
7	11.29	11.23	24	74.56	74.73	41	163.39	161.22
8	15.71	15.65	25	75.85	74.91	42	163.72	163.79
9	16.09	16.07	26	76.29	76.44	43	164.98	165.15
10	17.21	17.06	27	77.26	76.72	44	167.33	166.56
11	22.27	22.11	28	94.44	93.72	45	186.95	186.63
12	25.84	25.65	29	95.8	95.06	46	187.51	187.28
13	31.93	31.75	30	98.83	98.25	47	203.89	202.53
14	34.13	33.79	31	118.93	119.48	48	207.3	204.96
15	34.72	34.65	32	123.98	123.66	49	207.85	205.13
16	35.77	35.52	33	124.2	123.7	50	213.4	211.94
17	43.34	43.21	34	133.52	134.44			
18	45.68	45.55	35	151.5	151.66			

of lower eigenvalue composed with inverses of the IFS mappings. For example, on the unit interval the eigenfunction $\cos \pi jkx$ is built out of j copies of the eigenfunction $\cos \pi kx$ miniaturized (composed with $x \to jx$) and appropriately glued together. This occurs for the standard Laplacian on SG, and also for the pentagasket[13] and a number of other fractals discussed in Berry *et al.*[4] If this occurs, it would mean that the ratio of the eigenvalues would be an integer power of $r_i\mu_i$. It is easy enough to test if this happens. In Table 12 we list the spectrum and the spectrum multiplied by $r_0\mu_0$ and $r_1\mu_1 = (r_0\mu_0)^2$ for the lattice case $(k_0, k_1, k_2) = (1, 2, 2)$ (same as in Table 1), highlighting values that occur in all three columns, at least approximately. We also note that certain patterns occur in the number of the

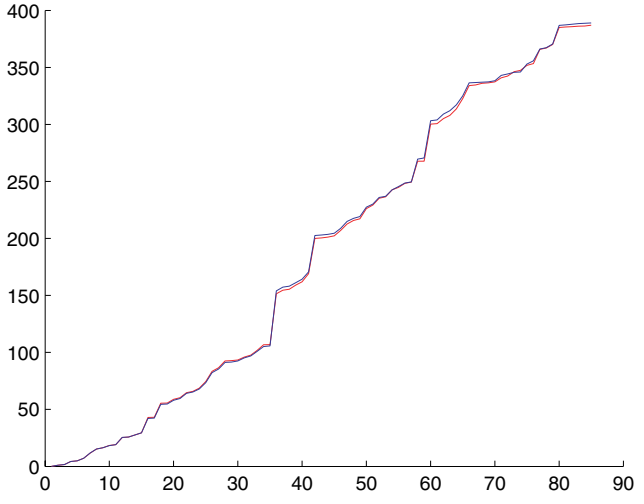

Fig. 18 Comparison of normalized eigenvalues for the outer approximation and FEM methods. Lattice case with $(k_0, k_1, k_2) = (1, 1, 2)$.

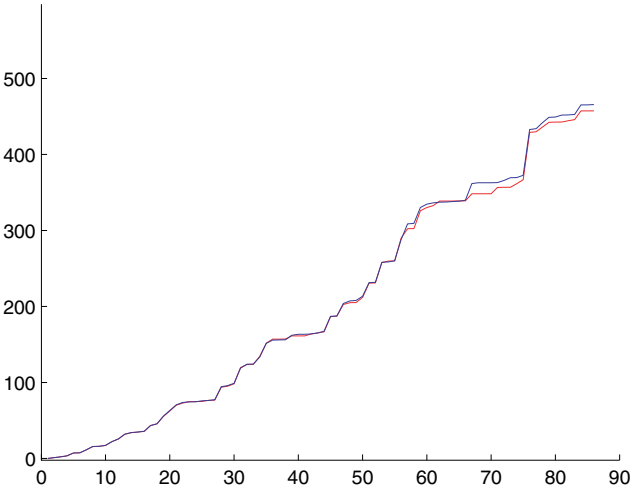

Fig. 19 Comparison of normalized eigenvalues for the outer approximation and FEM methods. Lattice case with $(k_0, k_1, k_2) = (1, 3, 3)$.

Table 10 Comparison of Normalized Eigenvalues for the Outer Approximation and FEM Methods. Nonlattice Case with $(r_0, r_1, r_2) = (0.8396, 0.4618, 0.4198)$.

k	$\overline{\lambda}_k$	λ_k	k	$\overline{\lambda}_k$	λ_k	k	$\overline{\lambda}_k$	λ_k
2	1	1	19	57.79	57.56	36	148.64	149.14
3	2.78	2.75	20	61.39	61.73	37	153.99	150.55
4	3.37	3.37	21	62.15	62.4	38	156.37	152.14
5	6.44	6.44	22	64.58	63.86	39	157.95	152.92
6	8.53	8.4	23	83.48	83.49	40	162.45	161.69
7	11.42	11.41	24	84.34	84.57	41	179.77	181.34
8	15.39	15.28	25	85.24	85.15	42	188.87	190.06
9	16.14	15.88	26	86.64	86.36	43	195.52	191.47
10	19.9	20.08	27	91.1	91.79	44	198.28	192.97
11	25.25	24.88	28	100.97	101.88	45	201.4	194.69
12	28.13	27.48	29	109.6	108.69	46	205.11	199.19
13	31.67	31.64	30	110.82	109.46	47	215.35	205.06
14	34.66	35.33	31	112.1	110.47	48	215.85	206.41
15	39.1	38.64	32	118.93	115.8	49	229.48	223.9
16	45.5	45.25	33	128.05	125.99	50	257.96	256.15
17	48.54	48.17	34	141.42	142.14			
18	49.69	49.6	35	147.33	146.9			

eigenvalues, as $\lambda_3, \lambda_6, \lambda_{12}, \lambda_{24}$ and $\lambda_{10}, \lambda_{20}, \lambda_{40}$. In other words, it appears that for certain choices of k we have

$$\lambda_{2^n k} \approx (r_0 \mu_0)^{-n} \lambda_k. \tag{5.2}$$

Is this an exact equality? Most likely not, as it is very reminiscent of the eigenvalue clusters (some clusters of different sizes appear here). But the data does not rule it out. However, we have looked at the associated eigenfunctions without finding any evidence of miniaturization. This is another question worth further investigation.

We are also interested in extremal problems associated with our classes of spectra and embeddings. Perhaps the simplest question is to describe the range of dimensions of our embeddings. The Hausdorff dimension of the embedding with parameters (ρ_0, ρ_1, ρ_2) is the unique solution of

$$\rho_0^d + \rho_1^d + \rho_2^d = 1. \tag{5.3}$$

We note that the limit as the triangle approaches a right triangle has $\rho_2 \to 0$ and $d \to 2$. So the supremum of all dimensions is 2, and is not an achieved

Table 11 Comparison of Normalized Eigenvalues for the Outer Approximation and FEM Methods. Non-Lattice Case with $(r_0, r_1, r_2) = (0.7684, 0.4994, 0.4994)$.

k	$\overline{\lambda}_k$	λ_k	k	$\overline{\lambda}_k$	λ_k	k	$\overline{\lambda}_k$	λ_k
2	1	1	19	52.08	52.29	36	140.5	142.36
3	1.88	1.88	20	56.8	56.99	37	145.21	148.94
4	3.42	3.42	21	64.52	64.71	38	146.29	149.9
5	6.92	6.89	22	65.88	65.99	39	155.38	157.82
6	7.98	8.03	23	70.93	71.36	40	158.21	161.65
7	10.23	10.18	24	73.19	73.56	41	164.65	167.07
8	15.32	15.12	25	75.36	76.07	42	170.26	170.36
9	16.25	16.2	26	86.92	84.69	43	171.05	170.47
10	18.38	18.57	27	95.93	94.67	44	175.92	176.26
11	19.19	19.54	28	97.19	95.73	45	184.92	188.88
12	22.42	22.67	29	97.24	99.81	46	186.08	189.59
13	29.9	29.83	30	102.37	101.48	47	197.16	196.09
14	33.03	32.84	31	102.9	103.13	48	206.6	211.94
15	37.13	36.56	32	104.06	103.9	49	208.12	212.79
16	41.41	41.09	33	118.47	121.16	50	225.2	221.09
17	42.44	43.1	34	129.61	132.04			
18	44.27	43.86	35	139.94	142.23			

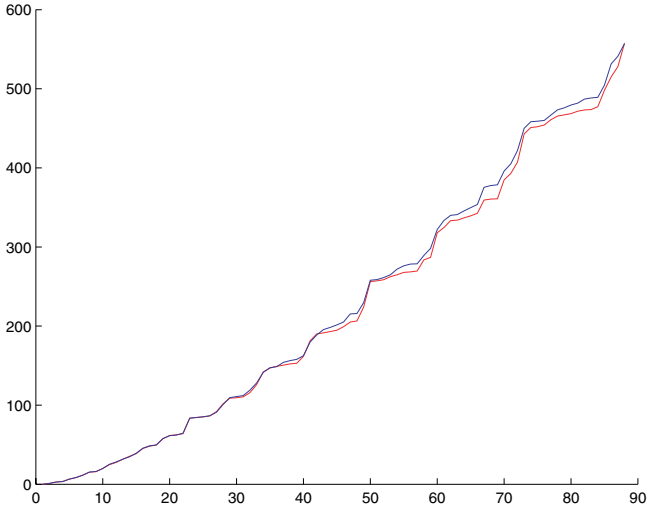

Fig. 20 Comparison of normalized eigenvalues for the outer approximation and FEM methods. Non-lattice case with $(r_0, r_1, r_2) = (0.8396, 0.4618, 0.4198)$.

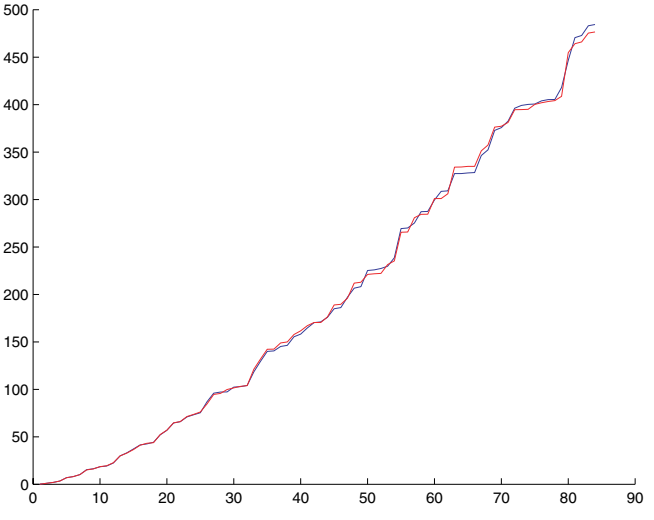

Fig. 21 Comparison of normalized eigenvalues for the outer approximation and FEM methods. Non-lattice case with $(r_0, r_1, r_2) = (0.7684, 0.4994, 0.4994)$.

maximum. If we choose angles $(2t, \frac{\pi}{2} - t, \frac{\pi}{2} - t)$ for the triangle and let $t \to 0$, the fractal approaches the interval, which has dimension 1, but the limit of d is still 2. This simply means that the dimension is a discontinuous function of the parameters at the point $\rho_0 = 1, \rho_1 = \rho_2$. The minimum dimension is $\log 3 / \log 2$, and it is achieved at the standard embedding $\rho_0 = \rho_1 = \rho_2 = 1/2$. We sketch a proof to show that d has a unique critical point. Since the ρ values are constrained by (1.19), which we abbreviate $F(\rho) = 1$, the method of Lagrange multipliers implies that ∇d is proportional to ∇F at a critical point. Differentiating (5.3) we obtain

$$\left(\sum_{i=0}^{2} \rho_i^d \log \rho_i \right) \frac{\partial d}{\partial \rho_j} + d\rho_j^{d-1} = 0 \quad \text{for } j = 0, 1, 2, \tag{5.4}$$

Table 12 The Spectrum of the Lattice Case $(k_0, k_1, k_2) = (1, 2, 2)$ and the Spectrum Multiplied by $r_0\mu_0$ and $r_1\mu_1 = (r_0\mu_0)^2$. Values are Highlighted that Occur in all Three Columns, at Least Approximately.

k	λ_k	$\lambda_k r_0\mu_0$	$\lambda_k r_1\mu_1$	k	λ_k	$\lambda_k r_0\mu_0$	$\lambda_k r_1\mu_1$	k	λ_k	$\lambda_k r_0\mu_0$	$\lambda_k r_1\mu_1$
2	17.8745	6.4947	2.3598	19	905.7363	329.0979	119.5781	36	2190.6595	795.9727	289.2177
3	28.2449	10.2628	3.729	20	909.2483	330.3739	120.0418	37	2193.4158	796.9742	289.5816
4	**65.1547**	23.6738	8.6019	21	991.709	**360.3359**	130.9285	38	2196.2594	798.0074	289.957
5	115.3914	41.9273	15.2343	22	1230.4227	447.0722	162.4443	39	2630.0976	955.6419	347.2337
6	146.6465	53.2838	19.3607	23	1267.7449	460.6332	167.3717	40	2659.7548	966.4178	351.1492
7	**180.6961**	**65.6557**	23.8561	24	1318.1156	478.9352	174.0217	41	2714.5052	986.3113	**358.3775**
8	220.2771	80.0373	29.0817	25	1364.0973	**495.6426**	**180.0924**	42	2758.2735	1002.2144	364.1559
9	264.0132	95.9288	34.8558	26	1387.9555	504.3115	183.2422	43	2802.87	1018.4185	370.0437
10	275.0242	99.9296	36.3096	27	1464.1403	531.9931	193.3004	44	3550.5921	1290.1022	468.7603
11	**357.3041**	129.8259	47.1724	28	1784.7991	648.504	235.6348	45	3608.9404	1311.3029	476.4636
12	474.8452	172.5343	62.6906	29	1793.7011	651.7385	236.81	46	3657.5568	1328.9676	482.8821
13	**494.8644**	**179.8082**	**65.3335**	30	1867.8102	678.666	246.5942	47	3661.0604	1330.2407	483.3447
14	531.7586	193.2137	70.2044	31	1878.7249	682.6318	248.0351	48	3751.8918	1363.2441	**495.3365**
15	678.6909	246.6013	89.6029	32	1910.7587	694.2712	252.2644	49	3757.4126	1365.2501	496.0654
16	694.1603	252.2221	91.6452	33	2055.6098	746.9027	271.388	50	3899.999	1417.0586	514.8901
17	795.7107	289.1203	105.0522	34	2056.1388	747.0948	271.4579				
18	797.2855	289.6925	105.2601	35	2188.9568	795.3541	288.9929				

which just says that $\{\frac{\partial d}{\partial \rho_j}\}$ is proportional to $\{\rho_j^{d-1}\}$. So the Lagrange condition is that $\{\rho_j^{d-1}\}$ is proportional to $\{\frac{\partial F}{\partial \rho_j}\}$, or

$$\rho_j^{1-d}\frac{\partial F}{\partial \rho_j} \text{ is independent of } j \tag{5.5}$$

at a critical point. Note that (5.5) obviously holds when $\rho_0 = \rho_1 = \rho_2$. Since $\frac{\partial F}{\partial \rho_j} = 2\rho_j + 2(\rho_0\rho_1\rho_2)/\rho_j$, we can write (5.5) as

$$f(\rho_0) = f(\rho_1) = f(\rho_2) \quad \text{for} \tag{5.6}$$

$$f(t) = 2t^{2-d} + 2(\rho_0\rho_1\rho_2)t^{-d}. \tag{5.7}$$

Note that for any fixed value of $\rho_0\rho_1\rho_2$, the function $f(t)$ has only one critical point, hence is at most two-to-one. So (5.6) can only hold if at least two of the ρ_j are equal (without loss of generality $\rho_1 = \rho_2$). In Fig. 25 we show the graph of d as a function of ρ_0 when $\rho_1 = \rho_2$, showing that it has a unique minimum when $\rho_0 = 1/2$ (hence $\rho_1 = \rho_2 = 1/2$).

A related question involves the extrema of the values α in (1.10) and β in (1.15). Note that

$$\beta = \alpha/(\alpha + 1) \tag{5.8}$$

so the answer is the same for both. Recall that α may be interpreted as the dimension of the fractal with respect to the resistance metric, and $\alpha + 1$ as

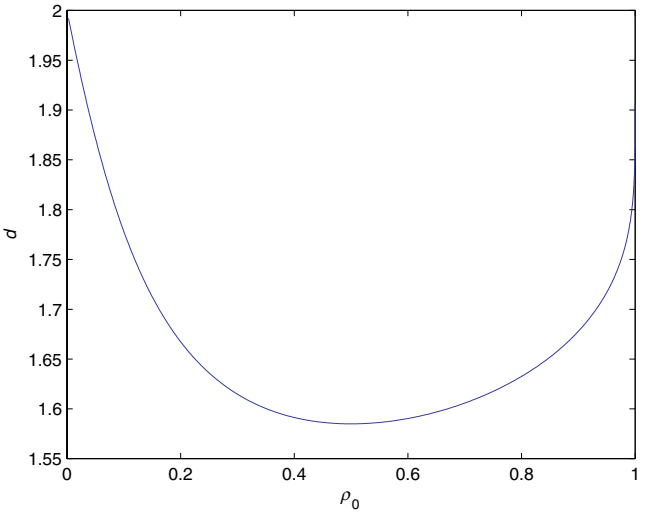

Fig. 22 d as a function of ρ_0 when $\rho_1 = \rho_2$.

the order of the Laplacian. Of course β controls the growth of the eigenvalues

$$\lambda_j \approx j^{1/\beta} \tag{5.9}$$

so smaller values of β make the eigenvalues larger (at least for large values of j).

We conjecture that the minimum values $\alpha_{\min} = \frac{\log 3}{\log 5 - \log 3} \approx 2.151$ and $\beta_{\min} = \frac{\log 3}{\log 5} \approx 0.683$ for the standard Laplacian with $r_0 = r_1 = r_2 = 3/5$, and there are no interior critical points. An argument similar to the above argument for the minimum of d should be possible, but because the equations for the algebraic variety of (r_0, r_1, r_2) values is very

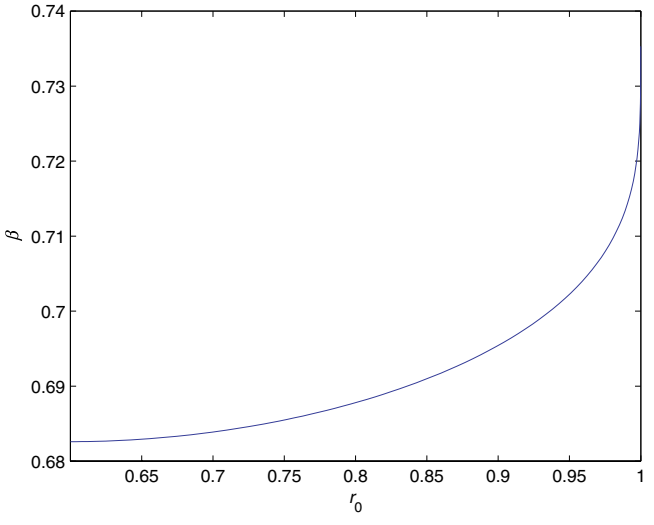

Fig. 23 β as a function of r_0 when $r_1 = r_2$.

complicated, we have not been able to carry out the details. In Fig. 23 we show that the graph of β as a function of r_0 when $r_1 = r_2$, and in Fig. 24 we show a rough sketch of the graph of β as a function of (r_0, r_1).

If the above conjecture is valid, the maximum value of α or β will not be attained, but we can compute the supremum. To do this we allow $r_2 = 0$. This does not correspond to any Laplacian, but we can still make sense of (1.11) as $r_0^\alpha + r_1^\alpha = 1$, where $(r_0, r_1, 0)$ lie on the same algebraic variety. In this case the equation simplifies to

$$e_2(-e_1^3 - e_1^2 + 4e_1e_2 + e_1 + 1) = 0 \tag{5.10}$$

where $e_1 = r_0 + r_1$ and $e_2 = r_0 r_1$ are the elementary symmetric polynomials. Again a Lagrange multiplier argument shows that the unique interior critical point is at the symmetric point $r_0 = r_1 = \frac{1+\sqrt{5}}{4}$. This time it is a maximum, so the supremum of α is

$$\alpha_{\max} = \frac{\log 2}{\log 4 - \log(1+\sqrt{5})} \approx 3.2706 \tag{5.11}$$

and so

$$\beta_{\max} = \frac{\log 2}{\log 8 - \log(1+\sqrt{5})} \approx 0.7658. \tag{5.12}$$

In Fig. 25 we show the graph of β as a function of r_0 along the boundary $r_2 = 0$. We can also ask what happens at the endpoints of the boundary, say when $r_1 = t$ tends to zero. Substituting the Taylor expansion $r_0 = 1 + at + bt^2 + ct^3 + o(t^3)$ in (5.10) yields $a = b = 0$ and $c = -1/4$, so (1.11) becomes

$$\left(1 - \frac{t^3}{4} + o(t^3)\right)^\alpha + t^\alpha = 1 \tag{5.13}$$

which implies

$$\lim_{t\to 0}\alpha = 3. \tag{5.14}$$

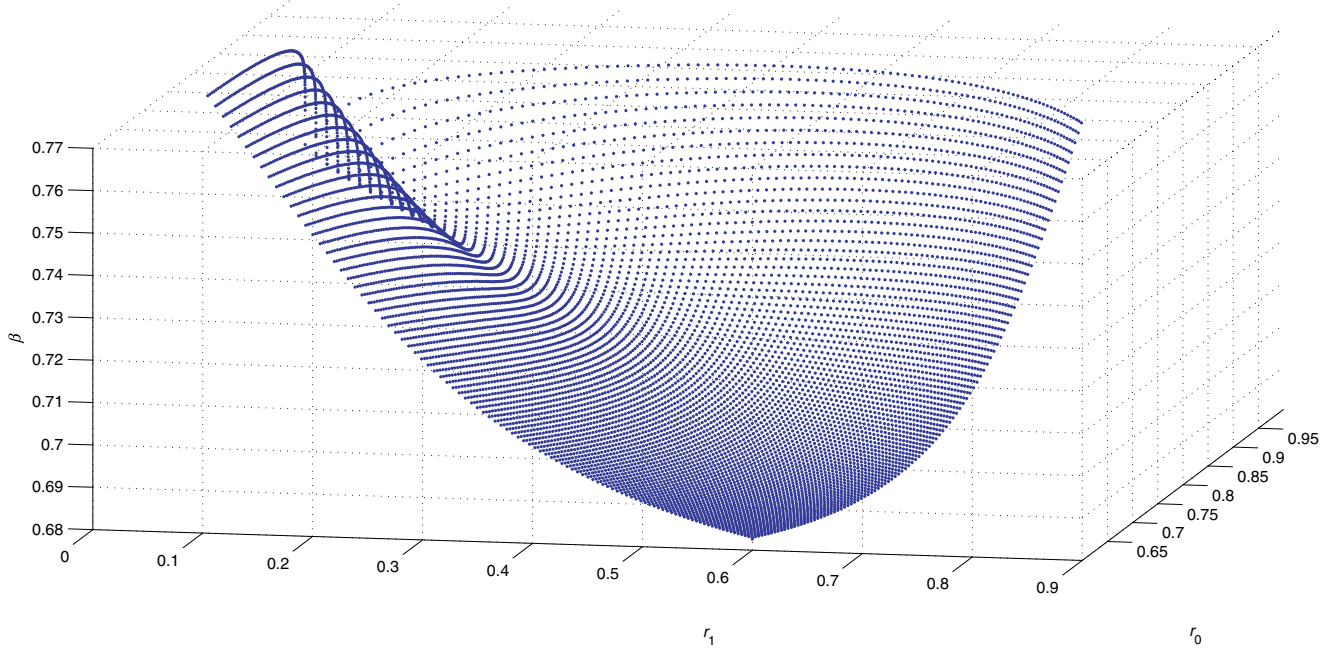

Fig. 24 β as a function of (r_0, r_1).

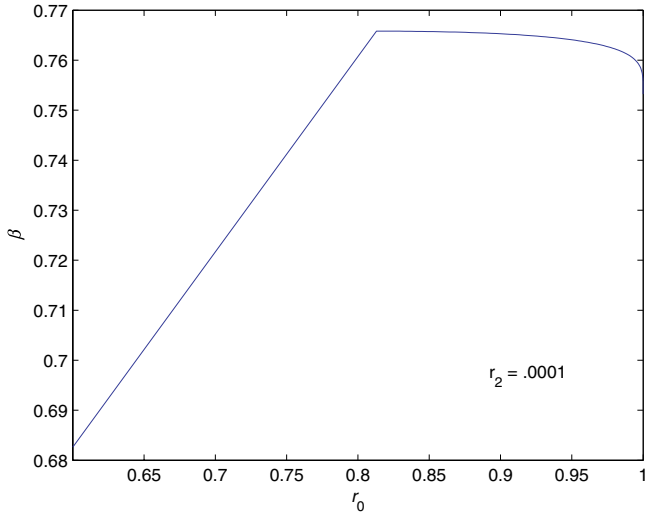

Fig. 25 β as a function of r_0 along the boundary $r_2 = 0$.

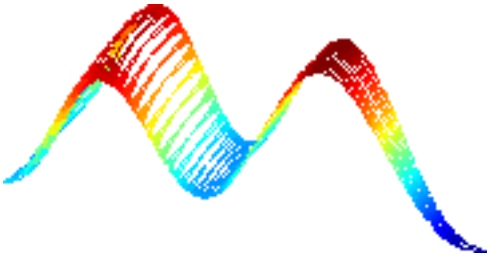

Fig. 26 Eigenfunction for fourth eigenvalue with $(r_0, r_1, r_2) = (0.8541, 0.4271, 0.4271)$.

Next we can look at extremal values of the renormalized eigenvalues λ_k for $k \geq 2$. The numerical evidence suggests that the maximum is not attained, but the supremum of the λ_k is k^2 and is approached as $r_1 = r_2$ tends to 0. Note that the values $\lambda_k = k^2$ occur for the second derivative Laplacian on the unit interval, and the embedded SG with $\rho_1 = \rho_2$ tending to 0 approaches an interval. Thus it appears that the spectrum of the Laplacian on SG with $r_1 = r_2$ converges to the spectrum of the Laplacian on the interval, even though β converges to 3/4 (the value of β on the unit interval is 1/2). This is another discontinuity, but there is no contradiction since the convergence of the spectra is not uniform. More evidence for this spectral convergence is that the eigenfunctions resemble cosine functions, as shown in Fig. 26.

In Figs. 27 to 34 we show the graphs of λ_k for $2 \leq k \leq 9$ as a function of r_1/r_0 and r_2/r_0. We have to restrict the domain to values above 0.2 since we lose accuracy for smaller values. We know that for large values of k, the standard Laplacian (here corresponding to $r_1/r_0 = r_2/r_0 = 1$) must be a local maximum for λ_k. We see this for $k = 9$. What is

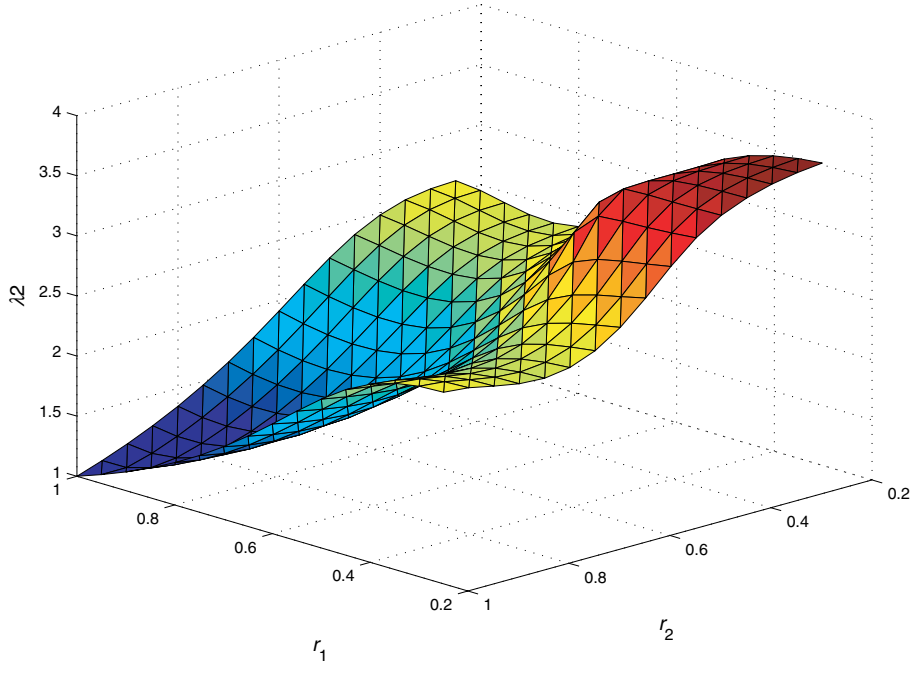

Fig. 27 λ_2.

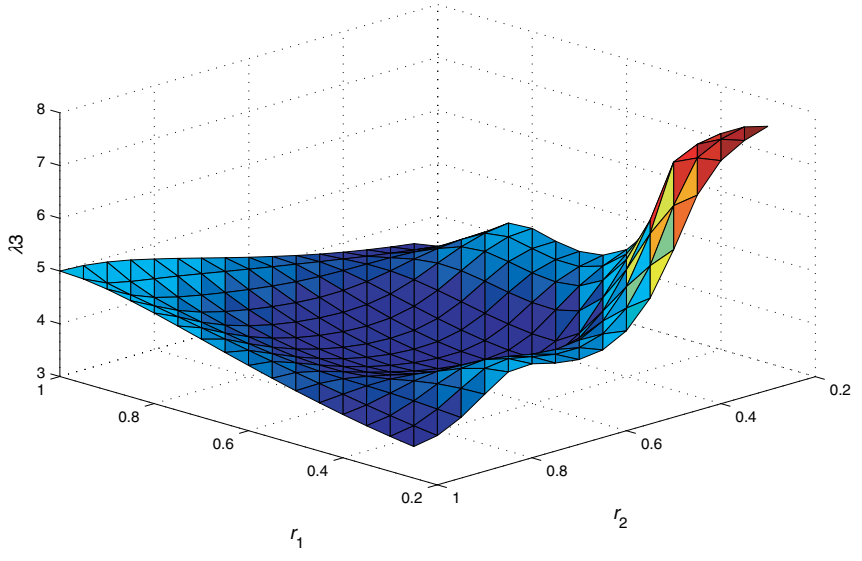

Fig. 28 λ_3.

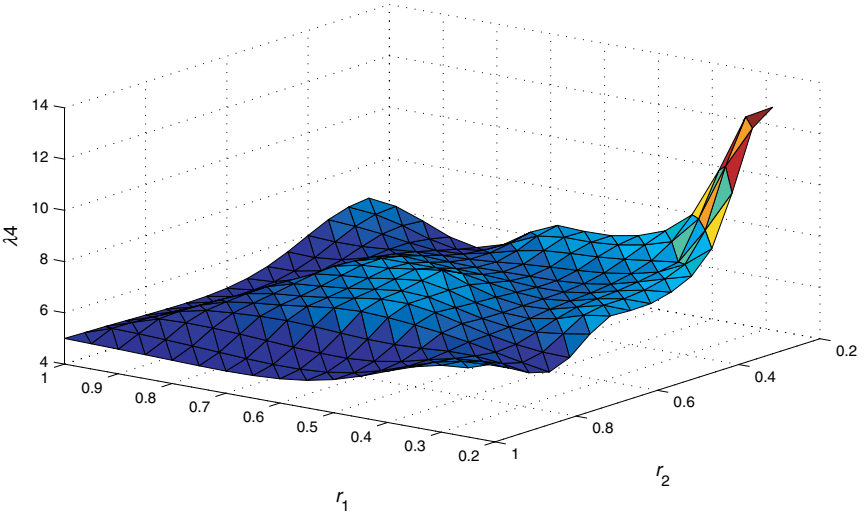

Fig. 29 λ_4.

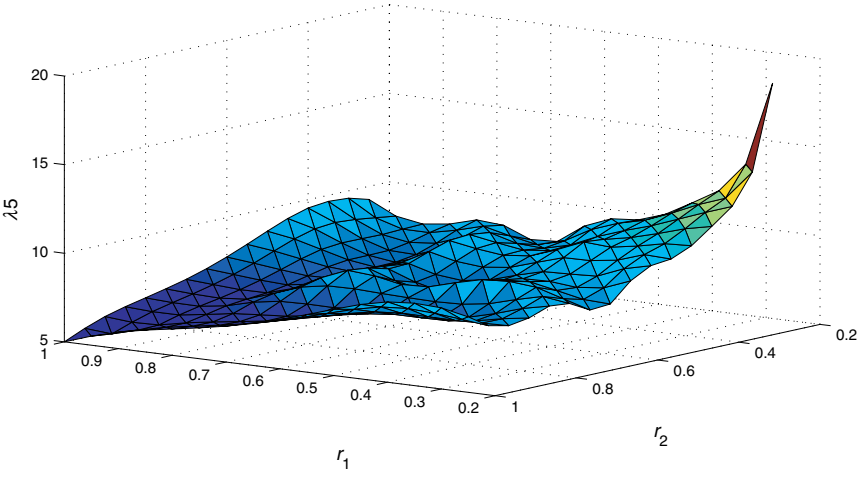

Fig. 30 λ_5.

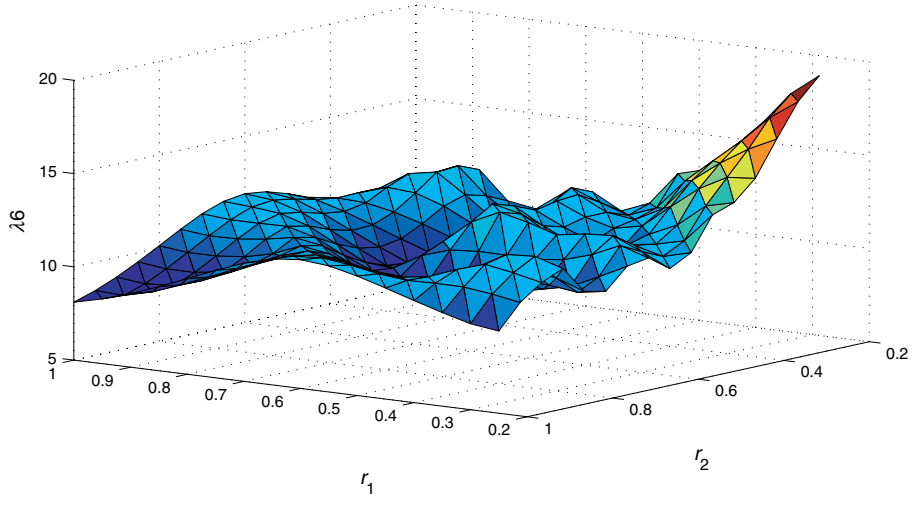

Fig. 31 λ_6.

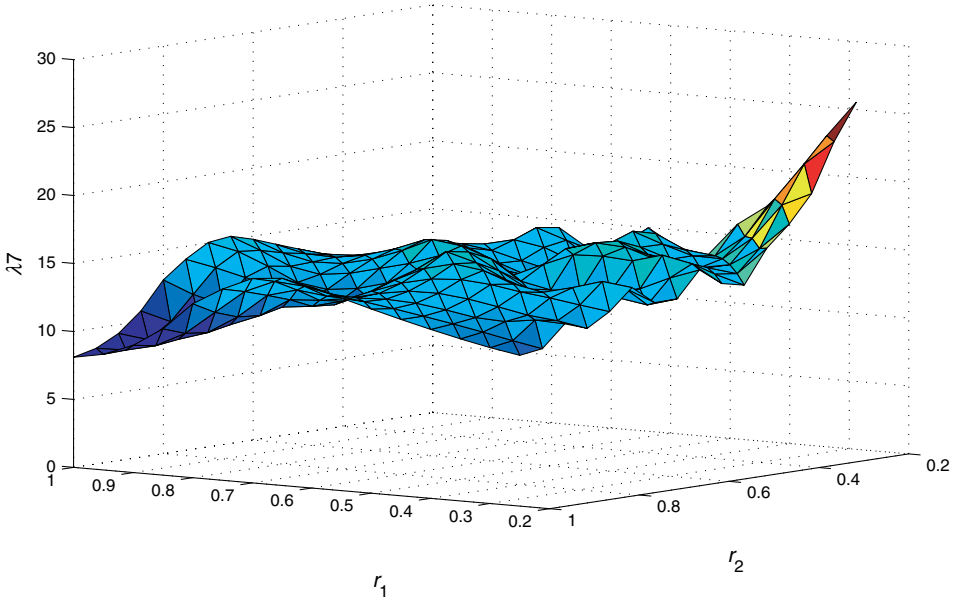

Fig. 32 λ_7.

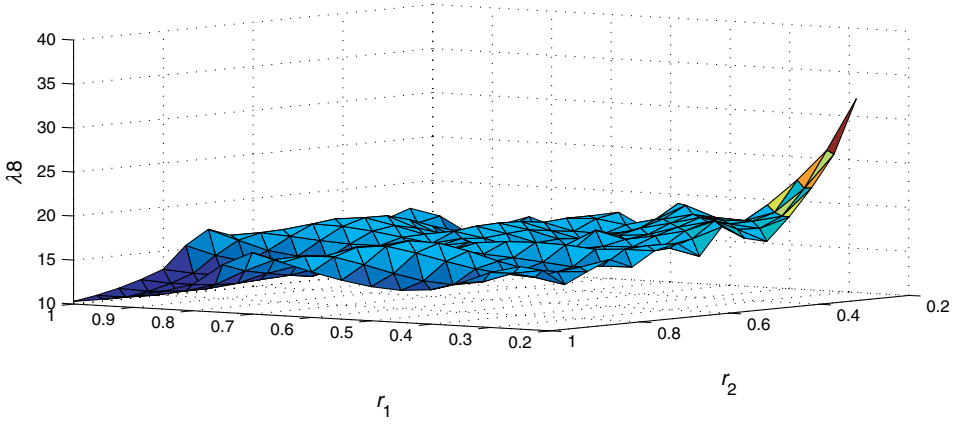

Fig. 33 λ_8.

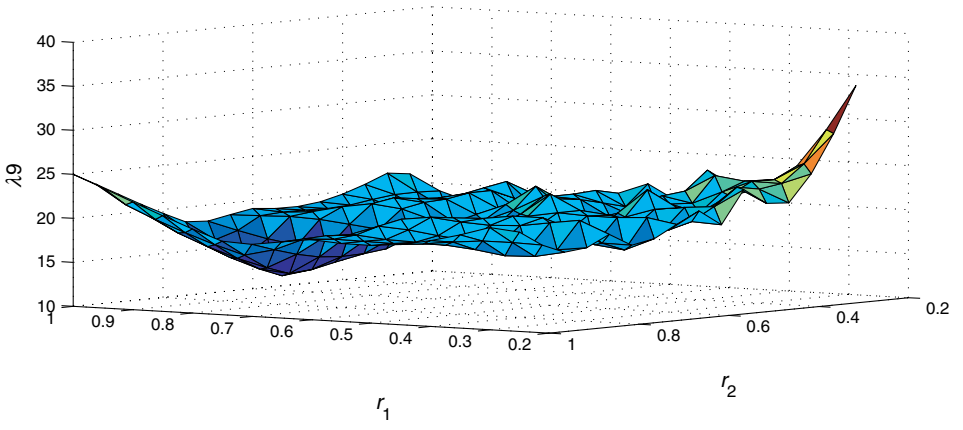

Fig. 34 λ_9.

Table 13 Global Minima.

λ_k	Minimum	r_0	r_1	r_2
2	1.0000	0.6	0.6	0.6
3	3.3253	0.8253	0.4539	0.4539
4	4.8697	0.6511	0.6511	0.4631
5	5.0000	0.6	0.6	0.6
6	8.1039	0.6	0.6	0.6
7	8.1039	0.6	0.6	0.6
8	10.3056	0.6	0.6	0.6
9	13.2478	0.6892	0.5514	0.5514

surprising is that for small values of k it is often a local minimum. Indeed, it appears to be the global minimum for $k = 2, 5, 6, 7, 8$. Table 13 gives the approximate global minima and the corresponding r values for $2 \leq k \leq 9$.

Acknowledgements

A. Blasiak's research is supported by the National Science Foundation through the Research Experiences for Undergraduates (REU) Program at Cornell, while R. S. Strichartz's research is supported in part by the National Science Foundation, grant DMS-0140194.

REFERENCES

1. J. Kigami, *Analysis on Fractals* (Cambridge University Press, 2001).
2. C. Sabot, Existence and uniqueness of diffusions on finitely ramified self-similar fractals, *Ann. Sci. Ecole Norm.* **30**(Suppl. 4) (1997) 605–673.
3. M. Cucuringu and R. Strichartz, Self-similar energy forms on the Sierpinski gasket with twists, *Potential Anal.* **27** (2007) 45–60.
4. T. Berry, S. Goff and R. Strichartz, Spectra of fractal Laplacians via outer approximation, in preparation.
5. R. Strichartz, Analysis on fractals, *Not. Am. Math. Soc.* **46** (1999) 1199–1208.
6. R. Strichartz, *Differential Equations on Fractals: A Tutorial* (Princeton University Press, 2006).
7. J. Kigami and L. Lapidus, Weyl's problem for the spectral distribution of Laplacians on p.c.f self-similar fractals, *Commun. Math. Phys.* **158** (1993) 93–125.
8. P. Kuchment and H. Zeng, Convergence of spectra of mesoscopic systems collaping onto a graph, *J. Math. Anal. Appl.* **258** (2001) 671–700.
9. M. Gibbons, A. Raj and R. Strichartz, The finite element method on the Sierpinski gasket, *Constructive Approx.* **17** (2001) 561–588.
10. R. Strichartz and M. Usher, Splines on fractals, *Math. Proc. Camb. Philas. Soc.* **129** (2000) 331–360.
11. M. Fukushima and T. Shima, On a spectral analysis for the Sierpinski gasket, *Potential Anal.* **1** (1992) 1–35.
12. M. Barlow and J. Kigami, Localized eigenfunctions of the Laplacian on p.c.f. self-similar sets, *J. Lond. Math. Soc.* **56** (1997) 320–332.
13. B. Adams, S. A. Smith, R. S. Strichartz and A. Teplyaev, The spectrum of the Laplacian on the pentagasket, *Trends in Mathematics: Fractals in Graz 2001* (Birkhauser, 2003), pp. 1–24.
14. T. Shima, On eigenvalue problems for Laplacians on p.c.f. self-similar sets, *Japan J. Ind. Appl. Math.* **13** (1996) 1–23.
15. R. Strichartz, Laplacians on fractals with spectral gaps have nicer Fourier series, *Math. Res. Lett.* **12** (2005) 269–274.
16. A. Fok and N. Kajino, in preparation.
17. T. Prosen and M. Robnik, Energy level statistics in the transition region between integrability

and chaos, *J. Phys. A Math. Gen.* **26** (1993) 2371–2387.
18. T. Prosen and M. Robnik, Numerical demonstration of the Berry-Robnik level spacing distribution, *J. Phys. A Math. Gen.* **27** (1994) L459–L466.
19. T. Prosen and M. Robnik, Semiclassical energy level statistics in the transition region between integrability and chaos: transition from Brody-like to Berry-Robnik behavior, *J. Phys. A Math. Gen.* **27** (1994) L459–L466.
20. A. Weinstein, Asymptotics of eigenvalue clusters for the Laplacian plus a potential, *Duke Math. J.* **44**(4) (1977) 883–892.
21. V. Guillemin, Some spectral results for the Laplace operator with potential on the n-sphere, *Adv. Math.* **27** (1978) 273–286.
22. K. Okoudjou and R. Strichartz, Asymptotics of eigenvalue clusters of Schrödenger operators on the Sierpinski gasket, *Proc. Am. Math. Soc.* **135** (2007) 2453–2459.